

4

Shock-Metamorphic Effects in Rocks and Minerals

4.1. FORMATION CONDITIONS AND GENERAL CHARACTERISTICS

The growing recognition since the 1960s of the geological importance of meteorite impact events, and the large number of impact structures still preserved on Earth, is largely the result of two related discoveries: (1) The extreme physical conditions that are imposed by intense shock waves on the rocks through which they pass produce unique, recognizable, and durable **shock-metamorphic effects**; (2) such shock waves are produced naturally only by the hypervelocity impacts of extraterrestrial objects (*French, 1968a, 1990b; French and Short, 1968*). Shock-metamorphic effects (also called “shock effects” or “shock features”) have been critical to the identification of terrestrial impact structures because of their uniqueness, wide distribution, ease of identification, and especially their ability to survive over long periods of geologic time.

With the acceptance of shock effects as a criterion for impact, the record of terrestrial impact events is no longer limited to small young structures that still preserve definite meteorite fragments. Equally convincing evidence for impact can now be provided by a wide variety of distinctive deformation effects in the rocks themselves, and it has become possible to identify numerous old impact structures from which weathering and erosion have removed all physical traces of the projectiles that formed them. The recognition of preserved shock effects has been the main factor behind the steady increase in the number of recognized impact structures since the 1960s (*Grieve, 1991; Grieve et al., 1995; Grieve and Pesonen, 1992, 1996*; for historical reviews, see *Hoyt, 1987; Mark, 1987*).

The approximate physical conditions that produce shock-deformation effects in natural rocks have been established by a combination of theoretical studies, artificial explosions

(both chemical and nuclear), and experiments with laboratory shock-wave devices (for details, see papers in *French and Short, 1968* and *Roddy et al., 1977*; also *Stöffler, 1972; Kieffer and Simonds, 1980; Melosh, 1989; Stöffler and Langenhorst, 1994*). Peak shock pressures produced in an impact event range from ≤ 2 GPa (≤ 20 kbar) near the final crater rim to >100 GPa (≥ 1000 kbar) near the impact point. These pressures, and the resulting shock-deformation effects, reflect conditions that are far outside the range of normal geological processes (Fig. 4.1, Table 4.1). In ordinary geological environments, pressures equivalent to those of typical shock waves are attained only under static conditions at depths of 75–1000 km within Earth, well below the shallow-crustal regions in which impact structures are formed.

Shock-wave pressures differ in other important ways from pressures produced by more normal geological processes. The application of shock-wave pressures is both sudden and brief. A shock wave traveling at several kilometers per second will traverse the volume of a mineral grain or a rock sample in microseconds, and both the onset and release of pressure are highly transient. Shock-deformation effects therefore reflect transient stress conditions, high strain rates, and rapid quenching that are inconsistent with the rates of normal geological processes (Table 4.1). In addition, shock waves deposit energy in the materials through which they pass. A particular shock pressure will produce a specific postshock temperature, which depends chiefly on the nature of the target material. These postshock temperatures increase with increasing shock pressure (see the P-T curve labeled “Shock metamorphism” in Fig. 4.1). For large shock pressures, the resulting temperatures are high enough to produce melting and even vaporization within the target.

The unique conditions of shock-wave environments produce unique effects in the affected rocks. The nature and intensity of the changes depend on the shock pressures

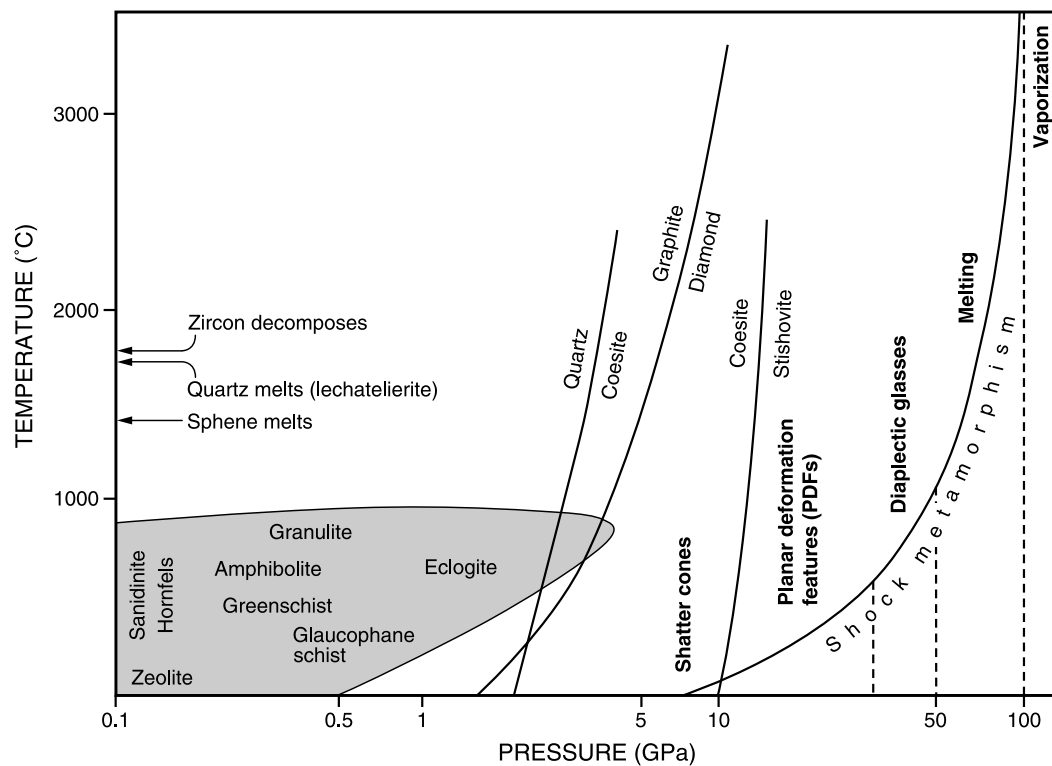


Fig. 4.1. Conditions of shock-metamorphism. Pressure-temperature plot showing comparative conditions for shock metamorphism and normal crustal metamorphism. [Note that the pressure axis (X-axis, in GPa) is logarithmic.] Shaded region at lower left ($P < 5$ GPa, $T < 1000^{\circ}\text{C}$) encloses the conventional facies (labeled) for crustal metamorphism. Shock-metamorphic conditions (at right) extend from ~ 7 to >100 GPa and are clearly distinct from normal metamorphic conditions. Approximate formation conditions for specific shock effects (labeled) are indicated by vertical dashed lines, and the exponential curve (“Shock metamorphism”) indicates the approximate postshock temperatures produced by specific shock pressures in granitic crystalline rocks. Relatively high shock pressures (>50 GPa) produce extreme temperatures, accompanied by unique mineral decomposition reactions (at left, near temperature axis). Stability curves for high-pressure minerals (coesite, diamond, stishovite) are shown for static equilibrium conditions; formation ranges under shock conditions may vary widely. (Adapted from *Stöffler*, 1971, Fig. 1; *Grieve*, 1990, p. 72; *Grieve and Pesonen*, 1992, Fig. 9.)

TABLE 4.1. Shock metamorphism: Distinction from other geological processes.

Characteristic	Regional and Contact Metamorphism; Igneous Petrogenesis	Shock Metamorphism
Geological setting	Widespread horizontal and vertical regions of Earth's crust, typically to depths of 10–50 km	Surface or near-surface regions of Earth's crust
Pressures	Typically $<1\text{--}3$ GPa	100–400 GPa near impact point; 10–60 GPa in large volumes of surrounding rock
Temperatures	Generally $\leq 1000^{\circ}\text{C}$	Up to $10,000^{\circ}\text{C}$ near impact point (vaporization); typically from 500° to 3000°C in much of surrounding rock
Strain rates	$10^{-3}/\text{s}$ to $10^{-6}/\text{s}$	$10^4/\text{s}$ to $10^6/\text{s}$
Time for completion of process	From $10^5\text{--}10^7$ yr	“Instantaneous”: Shock-wave passage through 10-cm distance, $<10^{-5}$ s; formation of large (100-km-diameter) structure <1 hr
Reaction times	Slow; minerals closely approach equilibrium	Rapid; abundant quenching and preservation of metastable minerals and glasses

TABLE 4.2. Shock pressures and effects.

Approximate Shock Pressure (GPa)	Estimated Postshock Temperature (°C)*	Effects
2–6	<100	Rock fracturing; breccia formation Shatter cones
5–7	100	Mineral fracturing: (0001) and {10 $\bar{1}$ 1} in quartz
8–10	100	Basal Brazil twins (0001)
10	100*	Quartz with PDFs {10 $\bar{1}$ 3}
12–15	150	Quartz → stishovite
13	150	Graphite → cubic diamond
20	170*	Quartz with PDFs {10 $\bar{1}$ 2}, etc. Quartz, feldspar with reduced refractive indexes, lowered birefringence
>30	275	Quartz → coesite
35	300	Diaplectic quartz, feldspar glasses
45	900	Normal (melted) feldspar glass (vesiculated)
60	>1500	Rock glasses, crystallized melt rocks (quenched from liquids)
80–100	>2500	Rock glasses (condensed from vapor)

* For dense nonporous rocks. For porous rocks (e.g., sandstones), postshock temperatures = 700°C (P = 10 GPa) and 1560°C (P = 20 GPa). Data from *Stöffler* (1984), Table 3; *Melosh* (1989), Table 3.2; *Stöffler and Langenhorst* (1994), Table 8, p. 175.

(Table 4.2). Lower shock pressures (~2–10 GPa) produce distinctive megascopic **shatter cones** in the target rocks (*Milton*, 1977; *Roddy and Davis*, 1977). Higher pressures (>10–45 GPa) produce distinctive high-pressure mineral polymorphs as well as unusual microscopic deformation features in such minerals as quartz and feldspar (*Stöffler*, 1972). Even higher pressures (≥50 GPa) produce partial to complete melting and even vaporization (≥100 GPa) of large volumes of the target rocks.

An especially distinctive and convincing form of evidence for meteorite impact is the suite of unique microscopic deformation features produced within individual minerals by higher-pressure (~10–45 GPa) shock waves. During the impact event, such pressures develop in target rocks near the center of the crater, and most of these rocks are immediately broken up and incorporated into the excavation flow that is being initiated by the expanding release wave (Figs. 3.4 and 3.5). As a result, these shock effects are found chiefly in individual target rock fragments in the breccias that fill the crater or in the ejecta deposited beyond the rim.

A wide variety of shock-produced microscopic deformation features has been identified in the minerals of shock-

metamorphosed rocks (for reviews, see *Chao*, 1967; papers in *French and Short*, 1968; *Stöffler*, 1972, 1974; *Stöffler and Langenhorst*, 1994; *Grieve et al.*, 1996). These include (1) **kink bands** in micas and (more rarely) in olivine and pyroxene; (2) several types of distinctive **planar microstructures** and related deformation effects in quartz, feldspar, and other minerals; (3) isotropic mineral glasses (**diaplectic** or **thetomorphic glasses**) produced selectively, most commonly from quartz and feldspar, without actual melting; (4) **selective melting** of individual minerals. Kink bands, although common in impact environments (Fig. 4.2), can also be produced by normal tectonic deformation; they are not a unique criterion for shock metamorphism, and they will not be discussed further. The other effects, particularly the distinctive planar microstructures in quartz and the diaplectic glasses, are now generally accepted as unique criteria for shock waves and meteorite impact events.

These shock-produced microscopic deformation features have several distinctive general characteristics. They are *pervasive*, and usually occur throughout a centimeter-sized rock sample, although they may be more erratically developed over larger distances (meters or tens of meters). They

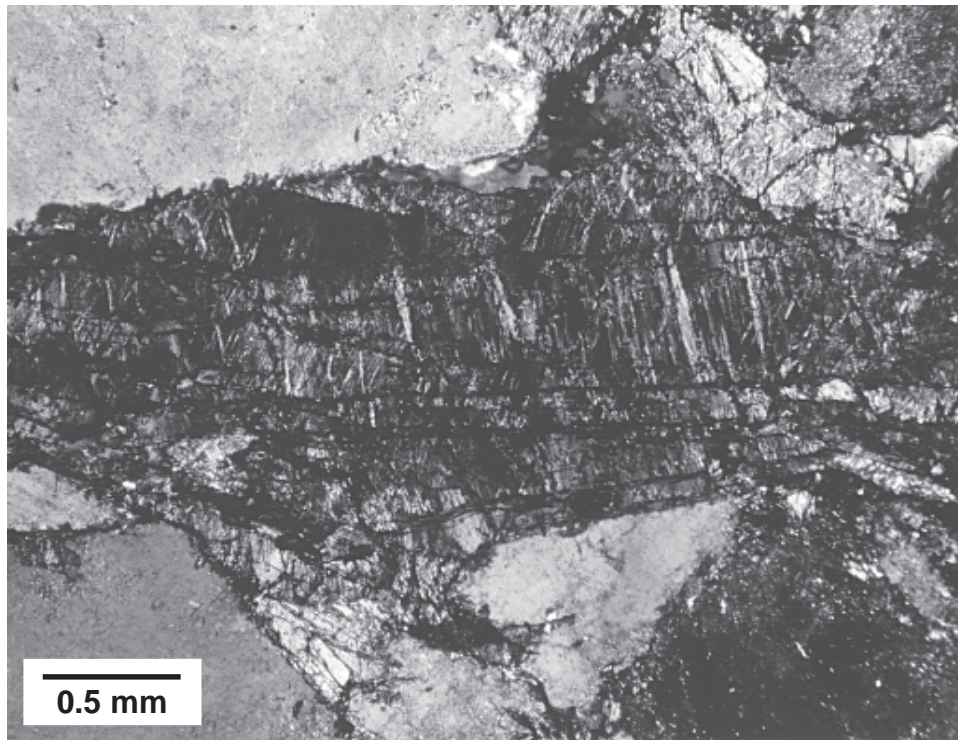


Fig. 4.2. Kink-banding; in biotite. Large biotite grain in basement granitic gneisses, northeast side of Sudbury structure (Canada), showing two sets of kink-banding at high angles to original cleavage (horizontal). Associated quartz (upper and lower left) and feldspar show no shock-deformation effects. Sample CSF-68-67 (cross-polarized light).

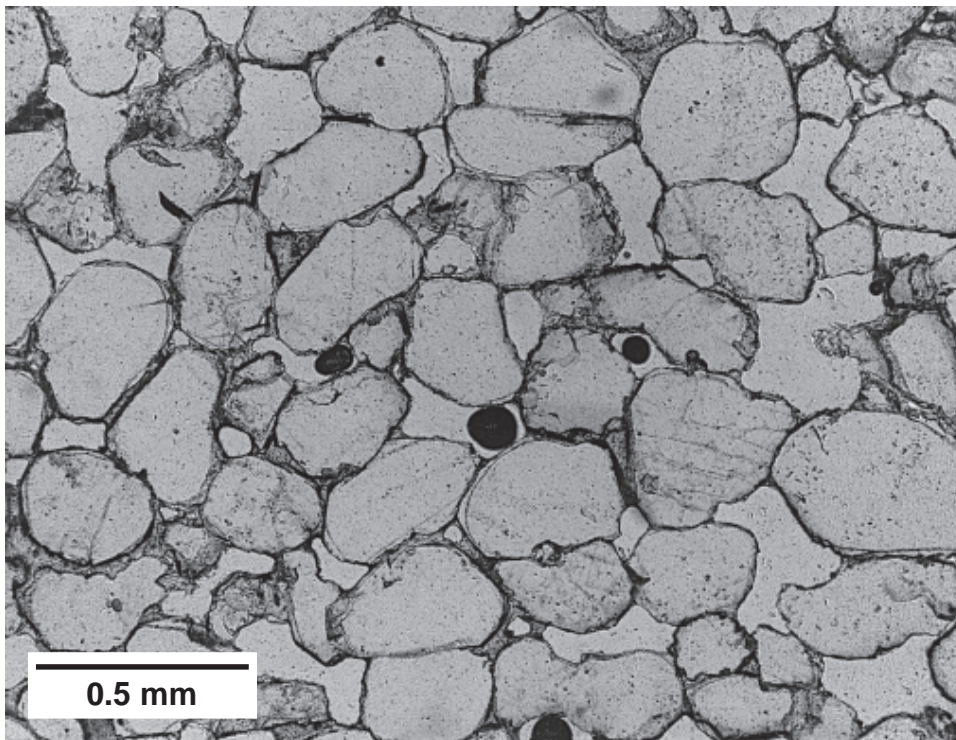


Fig. 4.3. Progressive shock metamorphism in sandstone (I). Unshocked Coconino Sandstone from the Barringer Meteor Crater (Arizona) is composed of well-sorted quartz grains with minor carbonate cement and pore space. The quartz grains are rounded to angular, clear, and undeformed; some grains display secondary overgrowths. (Black dots are bubbles in thin section mounting medium.) Ejecta sample from rim of crater. Sample MCF-64-4 (plane-polarized light).

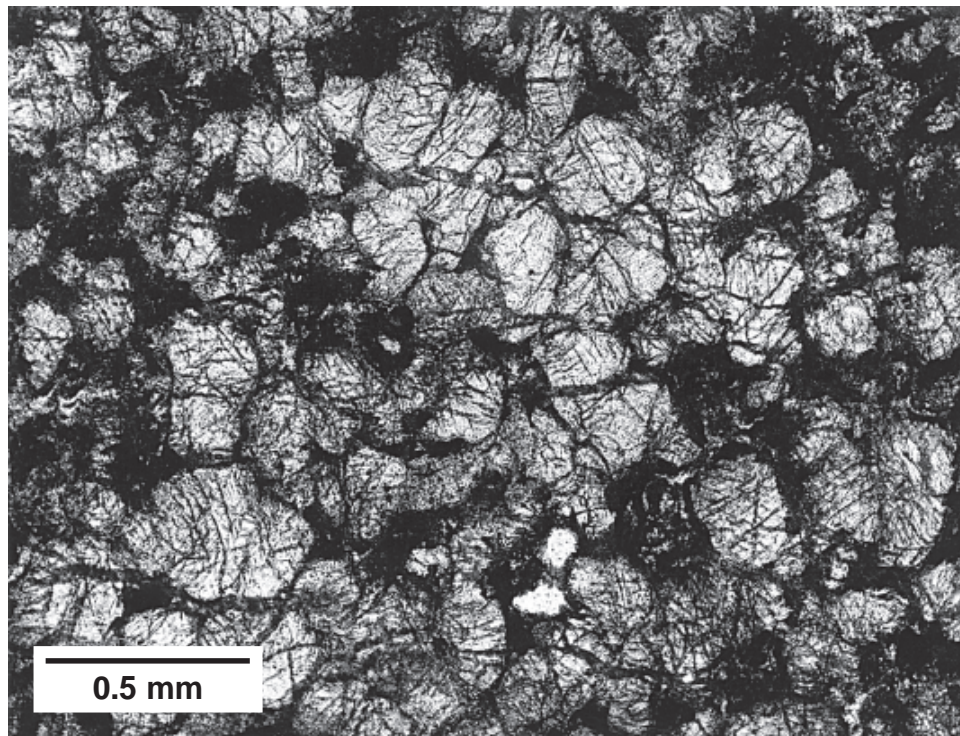


Fig. 4.4. Progressive shock metamorphism in sandstone (II). Moderately shocked Coconino Sandstone from the Barringer Meteor Crater (Arizona). The quartz grains are highly fractured and show numerous sets of subparallel fractures along cleavage planes. The original interstitial pore space has been collapsed and heated during passing of the shock wave, producing a filling of dark glass that frequently contains coesite. Ejecta sample from ground surface outside crater. Sample MCF-65-15-4 (plane-polarized light).

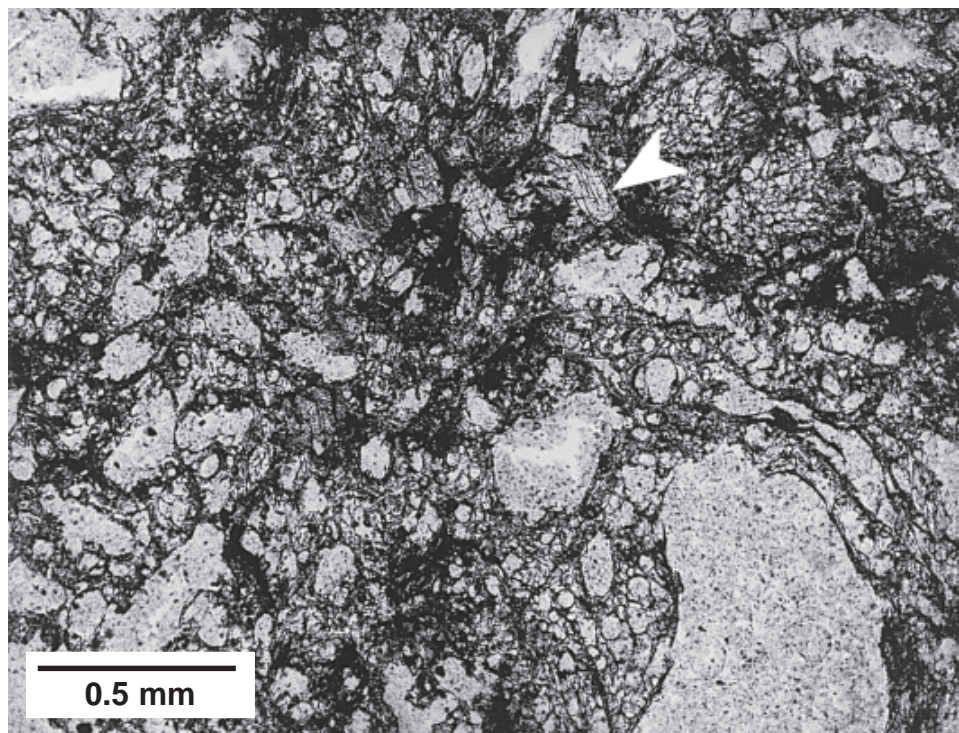


Fig. 4.5. Progressive shock metamorphism in sandstone (III). Highly shocked, melted, and vesiculated Coconino Sandstone from the Barringer Meteor Crater (Arizona). The original sandstone has been converted to a light, frothy, highly vesicular pumice-like material composed dominantly of nearly pure silica glass (*lechatelierite*). The vesicular glass contains a few remnant quartz grains (e.g., upper center, arrow) that are highly fractured and show development of distinctive PDFs in addition to the open cleavage cracks. Ejecta sample from ground surface outside crater. Sample MCF-65-11-2 (plane-polarized light).

are *mineralogically selective*; a given effect (e.g., isotropization) will occur in grains of a single mineral (e.g., quartz or feldspar), but not in grains of other minerals, even adjacent ones. Shock metamorphism is also characterized by a *progressive destruction of original textures* with increasing shock pressure, a process that eventually leads to complete melting or vaporization of the target rock (Figs. 4.3, 4.4, and 4.5).

4.2. STAGES OF SHOCK METAMORPHISM

The fact that different shock pressures produce a variety of distinctive shock features (Table 4.2) has made it possible to recognize different levels or **stages of shock metamorphism** (*Chao*, 1967; *Stöffler*, 1966, 1971, 1984; *von Engelhardt and Stöffler*, 1968; *Stöffler and Langenhorst*, 1994). These *stages* are not equivalent to the different *facies* recognized in normal metamorphism, because shock metamorphism is a rapid and nonequilibrium process and many of the most distinctive features produced by shock waves (e.g., high-pressure minerals and diaplectic glasses) are metastable under normal geological conditions. Nevertheless, key shock features occur frequently and consistently in natural impact structures, and the production of the same features in experimental studies has made approximate pressure and temperature calibrations possible. As a result, the stages of shock metamorphism have become an important concept for field studies of impact structures and for using certain features as approximate shock-wave barometers.

Current classifications of shock-metamorphic stages are based almost entirely on features developed in nonporous, quartz-bearing, crystalline igneous and metamorphic rocks. These lithologies are abundant in many of the impact structures studied so far, and they develop a varied suite of shock features over a wide range of shock pressures. Individual classifications of shock-metamorphic stages in these rocks differ in details, but the following summary of distinctive shock features and their approximate shock pressures (based largely on *Stöffler*, 1966, 1971, 1984; *Stöffler and Langenhorst*, 1994) provides a useful classification based on field and petrographic characteristics. [Other effects observed with increasing shock pressure include decreases in refractive index and increasing structural disorder (**shock mosaicism**) in mineral grains; for details, see *Stöffler*, 1972, 1974; *Stöffler and Langenhorst*, 1994).] It should be remembered that estimated pressures are only approximate, and that the formation of a given shock effect will also reflect such individual factors as rock type, grain size, and other structural features. The shock effects observed, and the inferred stages of shock metamorphism, will be different for other rock types, especially for carbonates, basaltic rocks, and porous rocks of any type.

For nonporous crystalline rocks, the following stages have been distinguished (see Table 4.2):

<2 GPa

Fracturing and brecciation, without development of unique shock features (see Chapter 5).

>2 GPa to <30? GPa

Shatter cones. At lower pressures (2 to <10 GPa), occurring without distinctive microscopic deformation features. At higher pressures (10 to ≤30 GPa), shatter cones may also contain distinctive microdeformation features.

~8 GPa to 25 GPa

Microscopic planar deformation features in individual minerals, especially quartz and feldspar. It has been possible to subdivide this zone on the basis of different fabrics of deformation features in quartz (*Robertson et al.*, 1968; *Stöffler and Langenhorst*, 1994).

>25 GPa to 40 GPa

Transformation of individual minerals to amorphous phases (**diaplectic glasses**) without melting. These glasses are often accompanied by the formation of high-pressure mineral polymorphs.

>35 GPa to 60 GPa

Selective partial melting of individual minerals, typically feldspars. Increasing destruction of original textures.

>60 GPa to 100 GPa

Complete melting of all minerals to form a superheated rock melt (see Chapter 6).

>100 GPa

Complete rock vaporization. No preserved materials formed at this stage (e.g., by vaporization and subsequent condensation to glassy materials) have been definitely identified so far.

4.3. MEGASCOPIC SHOCK-DEFORMATION FEATURES: SHATTER CONES

Shatter cones are the only distinctive and unique shock-deformation feature that develops on a megascopic (hand specimen to outcrop) scale. Most accepted shock-metamorphic features are microscopic deformations produced at relatively high shock pressures (>10 GPa). Lower shock pressures (1–5 GPa) produce a variety of unusual fractured and brecciated rocks, but such rocks are so similar to rocks formed by normal tectonic or volcanic processes that their presence cannot be used as definite evidence for an impact event. However, such low shock pressures also generate distinctive conical fracturing patterns in the target rocks, and the resulting **shatter cones** have proven to be a reliable field criterion for identifying and studying impact structures (*Dietz*, 1947, 1959, 1963, 1968; *Milton et al.*, 1972, 1996a; *Roddy and Davis*, 1977; *Sharpton et al.*, 1996a; *Dressler and Sharpton*, 1997).

Shatter cones are distinctive curved, striated fractures that typically form partial to complete cones (Figs. 4.6 and 4.7). They are generally found in place in the rocks below the crater floor, usually in the central uplifts of complex impact structures, but they are also rarely observed in isolated rock



Fig. 4.6. Shatter cones; small, well-developed. Small, finely sculptured shatter cones, developed in fine-grained limestone from the Haughton structure (Canada). The cone surfaces show the typical divergence of striae away from the cone apex ("horsetailing"). Photograph courtesy of R. A. F. Grieve.

fragments in breccia units. Shatter cones occur as individuals or composite groups, and individual cones may range from millimeters to meters in length (Figs. 4.7, 4.8, and 4.9) (Dietz, 1968; Sharpton *et al.*, 1996a). Far more common, however, are partial cones or slightly curved surfaces with distinctive radiating striations ("horsetailing") on them (Fig. 4.10).

The details of shatter cone morphology are also distinctive. Smaller secondary ("parasitic") cones commonly occur on the surfaces of both complete and partial shatter cones, forming a unique composite or "nested" texture. The surfaces of shatter cones, and the striations on them, are definite positive/negative features. The striations are also directional; they appear to branch and radiate along the surface of the cone, forming a distinctive pattern in which the

acute angle of the intersection points toward the apex of the cone (Figs. 4.6, 4.8, and 4.10).

Shatter cones form in all kinds of target rocks: sandstones, shales, carbonates, and crystalline igneous and metamorphic rocks. The most delicate and well-formed cones form in fine-grained rocks, especially carbonates (Fig. 4.6). In coarser rocks, shatter cones are cruder, and their striations are larger, making the cones more difficult to recognize and distinguish from nonshock deformational features such as slickensides (Figs. 4.8 and 4.10).

Shatter cones, especially well-formed examples, are easy to distinguish from similar nonimpact features (see Table 4.3). Some shatter cone occurrences may superficially resemble the "cone-in-cone" structures produced during

lithification of carbonate-bearing clastic sediments. However, the cones in cone-in-cone features have their axes normal to the bedding of the host rocks and their apexes pointing down. Shatter cones generally point upward, and their axes may lie at any angle to the original bedding, depending on the preimpact orientation of the target rock and its location relative to the impact point. Furthermore, the occurrence of shatter cones in a variety of rock types, especially non-sedimentary ones, is a good indication of an impact origin. The horsetailing striations on shatter cone surfaces sometimes resemble *slickensides* formed on faults, especially when the surfaces are approximately flat (Figs. 4.8 and 4.10). However, unlike slickensides, shatter cone striations are nonparallel and often show strong radiation and directionality, so that it is easy to determine the direction of the cone apex.

Shatter cones are now generally accepted as unique indicators of shock pressures and meteorite impact. They are especially valuable in this role because they form at relatively low shock pressures (typically 2–10 GPa, but perhaps as high as 30 GPa) and therefore develop throughout a large volume of target rock below the crater floor. They are typically widely and intensely developed in exposed central uplifts of large structures. Shatter cones form in a wide range of rock types, they are resistant to subsequent metamorphism, and (when well developed) they can be easily and immediately recognized in the field. Frequently, an initial discovery of shatter cones has spurred the search for, and discovery of, a range of equally definite shock effects produced at even higher pressures.

For well-developed shatter cones, it is possible to measure the orientation of the cone axes and to statistically determine the varying orientations of shatter cones throughout an impact structure. Such measurements (e.g., *Manton, 1965; Guy-Bray et al., 1966; Milton et al., 1972, 1996a*) have provided strong support for the use of shatter cones



Fig 4.7. Shatter cones; large. Large shatter cone and crudely conical striated surfaces in Mississagi Quartzite from the South Range (Kelley Lake) of the Sudbury structure (Canada). Cone axes point upward and into the Sudbury Basin (toward viewer) at a high angle. Cone axes are nearly parallel to the original bedding in the quartzite, which dips steeply back and to the right.

Fig. 4.8. Shatter cone; huge, well-striated. A large shatter cone, 2–3 m long, in quartzite in the central uplift of the Gosses Bluff structure (Australia). The cone axis plunges gently to the left, nearly normal to the original bedding in the quartzite, which appears as parallel joints dipping steeply to the right. Despite the crudeness of the large cone, the direction of the apex (right), parasitic cones, and distinctive horsetailing are all visible. Scale rule (at top) is 15 cm long.





Fig. 4.9. Shatter cone; huge. Unusually large shatter cone (megacone) (light-colored area, center) exposed in a cliff along a wave-cut shoreline on Patterson Island, one of the islands in the Slate Islands impact structure, Lake Superior (Canada). The huge cone, developed in Archean felsic metavolcanic rocks, points nearly straight up and is at least 10 m in length. At the exposed base, the exposed surface of the cone is at least 7 m wide. Only $\sim 25^\circ$ of the cone's basal perimeter is exposed, indicating that the true width of the feature may exceed 20 m at its base. Horsetail striations and parasitic cones cover all exposed surfaces. Several other large, conical features are obvious on the near-vertical cliff, but because of the steep scree-covered slopes these features have not yet been examined in detail. Photograph courtesy of V. L. Sharpton.



Fig. 4.10. Shatter cones; crude, striated surfaces. Poorly developed shatter cones in Serpent Quartzite, Sudbury (Canada). The cones are only partially developed, appearing as curved and striated surfaces. Divergence of the striae indicates that the cone apexes are to the right. Pen (at center) is 12 cm long.

TABLE 4.3. Shatter cones: Distinction from other geological features.

Cone-in-Cone	Shatter Cones
Conical secondary growth features formed during diagenesis; found in undisturbed sedimentary rocks.	Conical fracture features formed by transient shock waves ($P \sim 2$ to >10 GPa) and found in meteorite impact structures, typically in uplifted central rocks.
Restricted to carbonate-bearing rocks (limestones, limy shales); associated with secondary carbonate.	Found in all rock types (sedimentary, igneous, metamorphic). Best developed in fine-grained rocks, especially limestones.
Cone axes normal to bedding planes.	Cone axes oriented at any angle to bedding, depending on orientation of rock at time of impact and on postimpact movements.
Cones oriented point-down.	Cones originally form pointing in direction of source of shock wave, i.e., inward and upward. Orientation varies over structure. Orientation further modified by development of central uplift or later postcrater deformation. When beds restored to original horizontal position, cones point toward a focus above original surface, indicating external source of shock wave.
Striations along cone surface generally continuous, uniform.	Striations along cone surface typically show development of divergent radiations ("horsetailing") along surface. Development of secondary (parasitic) cones on main cone is typical.
Cone surfaces are growth surfaces against other cones or fine matrix in rock.	Cone surfaces are actual fracture surfaces; rock splits into new shatter-coned surfaces along cone boundaries. Unlike <i>slickensides</i> , striated cone surfaces show no relative motion, fit together without displacement.
Rocks typically show no deformation, metamorphism.	Frequently contain kink-banded micas or quartz (coarser grains) with shock-produced planar deformation features (PDFs).

as a criterion for impact. In several impact structures that formed in originally flat-lying sediments, the apexes of shatter cones in the rocks point inward and upward when the rocks are graphically restored to their original horizontal pre-impact position, indicating that the source of the shock wave that produced the shatter cones was located above the original ground surface (Guy-Bray *et al.*, 1966; Dietz, 1968; Manton, 1965; Howard and Offield, 1968; Wilshire *et al.*, 1972; Milton *et al.*, 1972, 1996a). More recently, shatter cones in the Beaverhead (Idaho) structure (Hargraves *et al.*, 1990) have been used to reconstruct the original shape and size of a large, ancient impact structure that was subsequently dissected and redistributed by major faulting during the Laramide Orogeny.

The use of shatter cones to identify impact structures requires caution, especially in cases where no other shock effects can be identified. Poorly developed shatter cones (Figs. 4.8 and 4.10) can be easily confused with normal fractures and slickensides, and the latter may be misidentified as shatter cones. Even in well-established impact structures, shatter cones may be entirely absent or poorly developed, or their orientations may be locally diverse and ambiguous (Fig. 4.11). Detailed studies of shatter cone orientations need to be done at more impact structures where they are well developed, but such studies need to be done with care (see, e.g., Manton, 1965; Milton *et al.*, 1972, 1996a).

It is a paradox that, even though shatter cones are a proven and valuable indicator of shock metamorphism and impact structures, the exact mechanisms by which the radiating

shock wave interacts with the target rock to generate shatter cones have not been studied in great detail and are still not understood (e.g., Dietz, 1968; Gash, 1971; Milton, 1977; Sharpton *et al.*, 1996a). A further complication in shatter cone formation is the evidence that, although the cones themselves form at relatively low shock pressures, localized melting and glass formation can occur along the cone surfaces, probably as the result of a complex combination of shock and frictional mechanisms (Gay, 1976; Gay *et al.*, 1978; Gibson and Spray, 1998). Combined theoretical, experimental, and field studies to understand the exact conditions of shatter cone formation are a major challenge for the future.

4.4. HIGH-PRESSURE MINERAL POLYMORPHS

When subjected to impact-produced shock waves, some minerals in target rocks (e.g., quartz, graphite) may transform to high-pressure minerals, just as they do under high static pressures produced in laboratory experiments or deep in Earth's crust. Graphite (C) can be converted to **diamond**. Quartz can be converted to **stishovite** at shock pressures of >12 – 15 GPa and to **coesite** at >30 GPa (Stöffler and Langenhorst, 1994). [These numbers illustrate one of the many differences between shock processes and normal geological deformation. Under conditions of static equilibrium, where reaction rates are slower and kinetic factors less im-



Fig. 4.11. Shatter cones; small, diversely oriented. This specimen shows a group of small, well-developed shatter cones, formed in a sample of Precambrian crystalline target rock at the Slate Islands structure (Canada). The cones show two distinct orientations, and cone axes appear to diverge above and below the coin. This type of diverse orientation may reflect small-scale nonuniformities in the shock waves, produced by local heterogeneities (bedding planes, joints, etc.) in the rock sample. Coin is about 2 cm in diameter. Photograph courtesy of V. L. Sharpton.

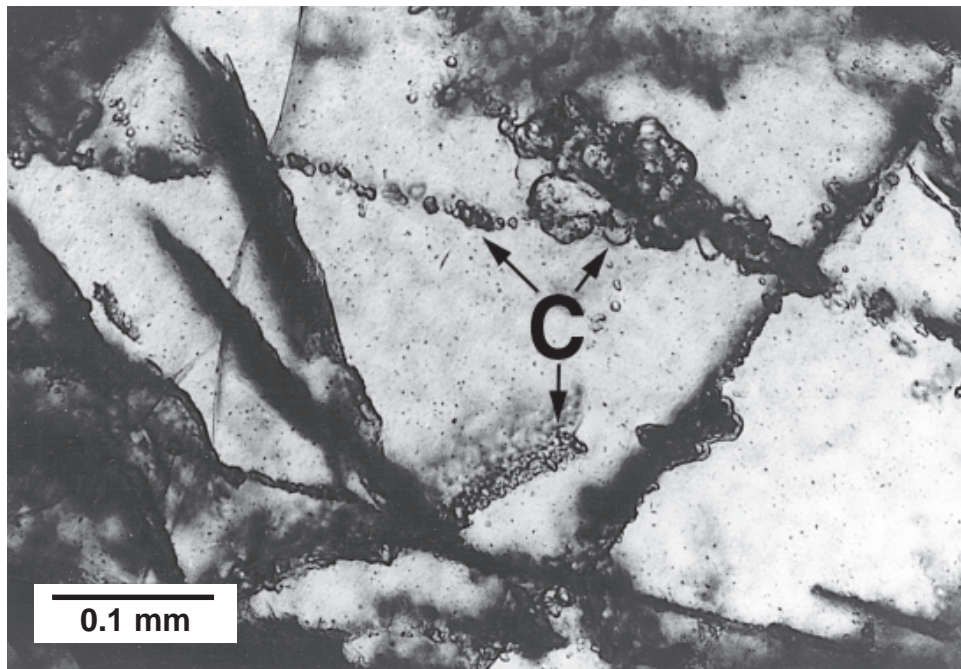


Fig. 4.12. Diaplectic quartz glass; with coesite. Diaplectic quartz glass (clear), with strings of small, high-relief crystals of coesite ("C"). From biotite granite inclusion in suevite breccia, Aufhausen, Ries Crater (Germany). Photograph courtesy of W. von Engelhardt (plane-polarized light).

portant, coesite forms from quartz at lower pressures (>2 GPa) than does stishovite (10–15 GPa).]

The identification of coesite and stishovite at several sites in the early 1960s provided one of the earliest criteria for establishing the impact origin of several structures, most notably the Ries Crater (Germany) (*Chao et al.*, 1960; *Shoemaker and Chao*, 1961) (Fig. 4.12). Most subsequent identifications of impact structures have been based on shock-produced **planar deformation features (PDFs)** in quartz, which are more widely distributed and simpler to identify. However, the discovery of both coesite and stishovite in the ancient Vredefort structure (South Africa) (*Martini*, 1991) was an important step in the growing acceptance of this structure as an impact site. Diamond and other high-pressure carbon compounds [e.g., **lonsdaleite** (hexagonal diamond)] produced from graphite in the shocked target rocks have also been identified at an increasing number of impact structures (*Masaitis*, 1998; *Masaitis et al.*, 1972; *Hough et al.*, 1995; *Koeberl et al.*, 1997c).

Coesite, stishovite, and diamond, when they are found in near-surface rocks, are unique and reliable indicators of meteorite impact. None of these minerals has been identified, for example, as the result of explosive volcanic eruptions. The use of coesite and diamond as impact criteria does require some care, however, because both minerals also occur naturally in deep-seated (depth >60 km) terrestrial rocks, where they have formed in stable equilibrium at the high static pressures (>2 GPa) present at these depths. Both minerals may then be transported to Earth's surface: coesite by tectonic processes and diamond in fragments carried up by unusual mafic (*kimberlite*) volcanic eruptions. However, stishovite, formed only at pressures >10 GPa, has never been identified in a nonimpact setting. Such static pressures could be produced only at depths of 300–400 km within Earth. Furthermore, the occurrence of such high-pressure minerals as coesite, stishovite, or diamond in near-surface crustal rocks [e.g., coesite and stishovite in sandstone at Barringer Meteor Crater (Arizona)], particularly when they occur as a disequilibrium assemblage with other chemically equivalent minerals (e.g., coesite + stishovite + silica glass + quartz), is definite evidence for meteorite impact.

4.5. PLANAR MICROSTRUCTURES IN QUARTZ

Shock waves produce a variety of unusual microscopic planar features in quartz, feldspar, and other minerals. These features typically occur as sets of parallel deformation planes within individual crystals. The recognition and interpretation of these features, particularly those in quartz, as unique products of meteorite impact has been a critical factor in identifying most new impact structures, in recognizing the impact origin of large, ancient, or deeply eroded structures, and in demonstrating the role of meteorite impact in the K/T extinction event.

Distinctive planar features in quartz (SiO₂) have been one of the most widely applied criteria for recognizing impact

structures (for reviews, details, and literature references, see papers in *French and Short*, 1968; also *von Engelhardt and Bertsch*, 1969; *Stöffler and Langenhorst*, 1994; *Grieve et al.*, 1996). Quartz is an ideal mineral for this purpose. It is abundant in a wide range of sedimentary and crystalline rocks. It is stable over long periods of geologic time, and it resists change by alteration and metamorphism. It is an optically simple (*uniaxial*) mineral to study and to analyze on the Universal Stage (*U-stage*). In particular, it displays a variety of different planar features whose development can be correlated with shock pressure (Table 4.2) (*Hörz*, 1968; *Robertson et al.*, 1968; *Stöffler and Langenhorst*, 1994), and can thus be used as a shock barometer to reconstruct the shock-pressure distribution that existed within an impact structure during the impact event (*Robertson*, 1975; *Grieve and Robertson*, 1976; *Robertson and Grieve*, 1977; *Grieve et al.*, 1996; *Dressler et al.*, 1998).

The production and properties of planar microstructures in quartz have been studied intensely since the early 1960s by geological investigations, shock-wave experiments, and both optical and electron microscopy (papers in *French and Short*, 1968; also *Stöffler and Langenhorst*, 1994). It is now recognized that shock waves produce several kinds of planar microstructures in quartz, and their detailed characterization and interpretation has been — and still is — an active and much-debated problem (e.g., *Alexopoulos et al.*, 1988; *Sharpton and Grieve*, 1990). At present, two basic types of planar features can be recognized, **planar fractures** and **planar deformation features (PDFs)** (Table 4.2).

4.5.1. Planar Fractures

Planar fractures are parallel sets of multiple planar cracks or cleavages in the quartz grain; they develop at the lowest pressures characteristic of shock waves (~5–8 GPa) (Figs. 4.13 and 4.14). The fractures are typically 5–10 μm wide and spaced 15–20 μm or more apart in individual quartz grains. Similar cleavage also occurs rarely in quartz from non-impact settings, and therefore planar fractures cannot be used independently as a unique criterion for meteorite impact. However, the development of intense, widespread, and closely spaced planar fractures (Fig. 4.15) is strongly suggestive of shock, and such fractures are frequently accompanied in impact structures by other features clearly formed at higher shock pressures (*Robertson et al.*, 1968; *Stöffler and Langenhorst*, 1994; *Grieve et al.*, 1996; *French et al.*, 1997).

4.5.2. Planar Deformation Features (PDFs)

Planar deformation features (PDFs) is the designation currently used for the distinctive and long-studied shock-produced microstructures that were formerly given a variety of names (e.g., “planar features,” “shock lamellae”). In contrast to planar fractures, with which they may occur, PDFs are not open cracks. Instead, they occur as multiple sets of closed, extremely narrow, parallel planar regions (Fig. 4.16). Individual PDFs are both narrow (typically <2–3 μm) and more closely spaced (typically 2–10 μm) than planar fractures (Figs. 4.17 and 4.18). Detailed optical and TEM studies have shown that, within individual PDFs, the atomic

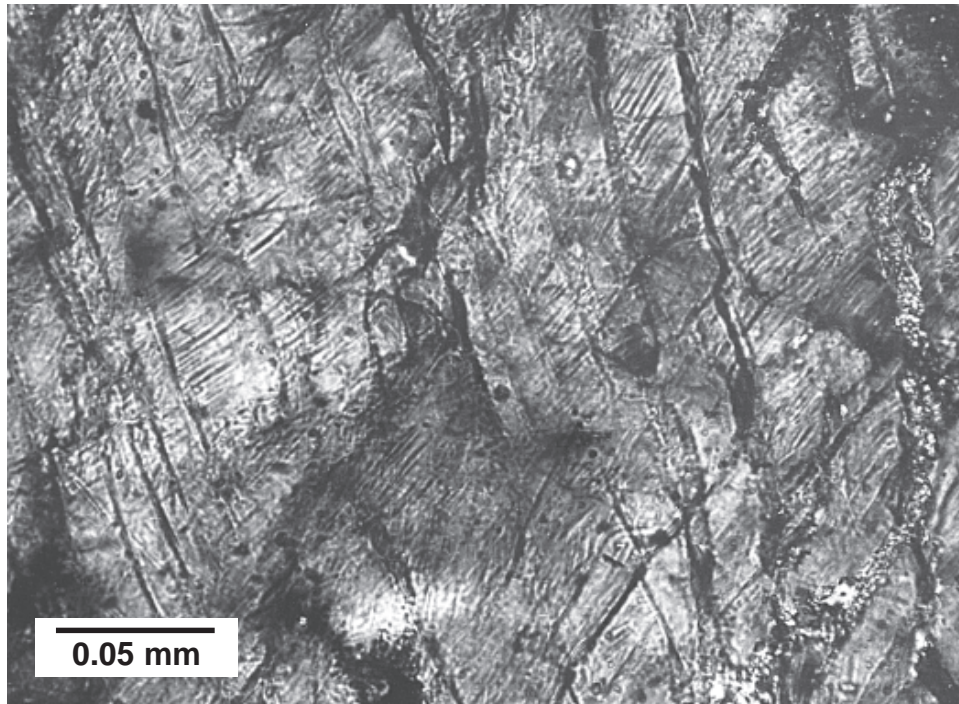


Fig. 4.13. Quartz; cleavage and PDFs. High-magnification view of relict deformed quartz grain in highly shocked and vesiculated Coconino Sandstone [Barringer Meteor Crater (Arizona)]. The quartz grain shows irregular, subparallel fractures (dark, near-vertical), combined with shorter cross-cutting light-and-dark planar features, possibly PDFs (upper right/lower left). Note the irregular extinction in the grain. Sample MCF-65-15-3 (cross-polarized light).

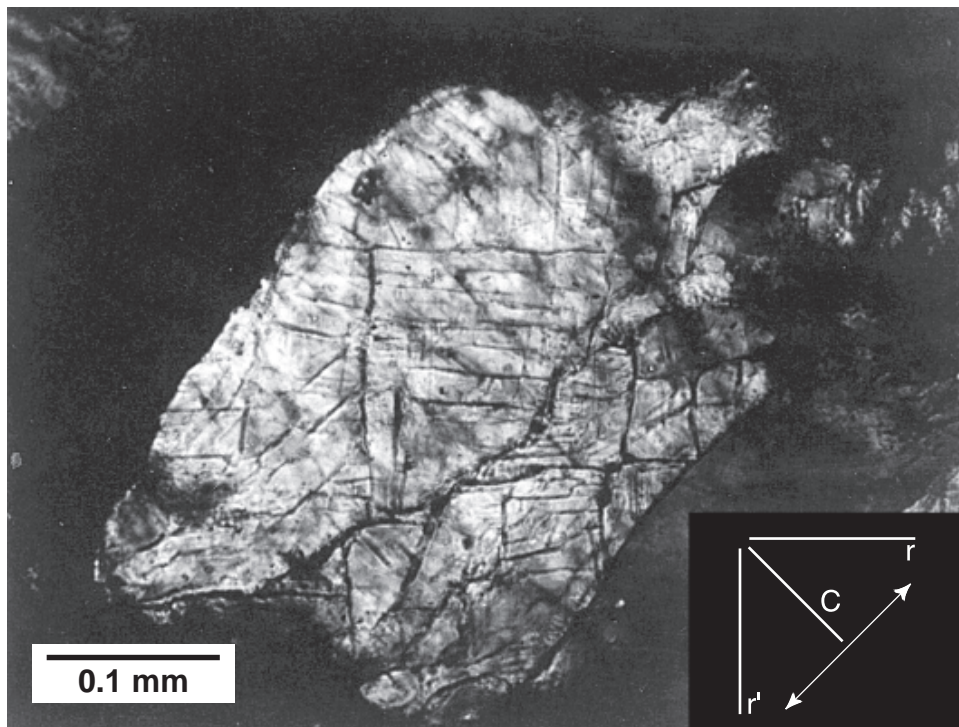


Fig. 4.14. Quartz; cleavage. Quartz grain in moderately shocked Coconino Sandstone from Barringer Meteor Crater (Arizona), showing irregular extinction and multiple sets of cleavage fractures parallel to $c(0001)$, $m\{10\bar{1}0\}$, $r\{10\bar{1}1\}$, and r' . c -axis direction (arrow) and directions of cleavage traces indicated in inset. Photograph courtesy of T. E. Bunch (cross-polarized light).

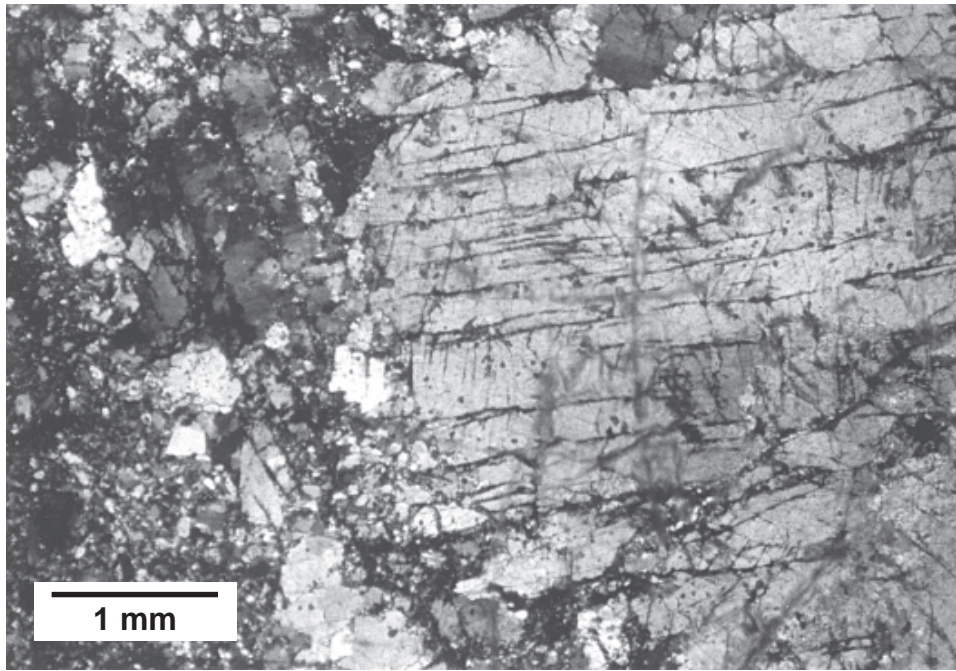


Fig. 4.15. Quartz; fractured, in quartzite. Intense fracturing of quartz in a coarse-grained metamorphosed orthoquartzite target rock from the Gardnos structure (Norway). The large quartz grain (right) grades into a finer-grained recrystallized shear zone (left). The quartz grain is cut by numerous subparallel planar fractures (longer, dark, subhorizontal lines) and by much shorter planar features (short, dark, near-vertical lines) that originate along the fracture planes. These latter features may be relicts of actual PDFs or of Brazil twins parallel to the base (0001). Within the Gardnos structure, the originally white quartzite is dark gray to black and highly fractured, and the fractures within the quartz grains contain carbonaceous material. Sample NG-94-17B (cross-polarized light).

structure of the original crystalline quartz is severely deformed, so that the quartz has been transformed into a distinct amorphous phase (Müller, 1969; Kieffer *et al.*, 1976a; Goltrant *et al.*, 1991, 1992).

The importance of PDFs arises from the fact that they are clearly distinct from deformation features produced in quartz by nonimpact processes, e.g., **cleavage** or **tectonic (metamorphic) deformation lamellae (Böhm lamellae)** (Carter, 1965, 1968; Alexopoulos *et al.*, 1988; Stöffler and Langenhorst, 1994). Cleavages are open fractures; they tend to be relatively thick ($\sim 10\ \mu\text{m}$) and widely spaced ($\geq 20\ \mu\text{m}$). Deformation lamellae consist of bands of quartz typically $10\text{--}20\ \mu\text{m}$ thick and $>10\ \mu\text{m}$ apart that are optically distinct and slightly misoriented relative to the host grain. In contrast to these features, shock-produced PDFs are narrow ($<2\text{--}3\ \mu\text{m}$) straight planes consisting of highly deformed or amorphous quartz, and they are generally oriented parallel to specific rational crystallographic planes in the host quartz crystal, especially to the base $c(0001)$ or to low-index rhombohedral planes such as $\omega\{10\bar{1}3\}$, $\pi\{10\bar{1}2\}$, and $r\{10\bar{1}1\}$ (Table 4.4).

The presence of well-developed PDFs produces a striking and distinctive appearance in thin section. Unaltered PDFs form multiple sets of continuous planes that extend across most or all of the host grain (Figs. 4.16, 4.17, and 4.18). These fresh, continuous PDFs tend to be observed only in unaltered material from shock-wave experiments and from younger, well-preserved impact structures, e.g., Barringer Meteor Crater (Arizona) (age 50 ka) (Fig. 4.13)

and the Ries Crater (Germany) (age 15 Ma) (Fig. 4.16). However, preservation of fresh, continuous PDFs depends on geological circumstances, including cooling rate and postimpact temperatures. Fresh, well-preserved PDFs are also present in older structures, e.g., Sierra Madera (Texas) (age $<100\ \text{Ma}$) (Fig. 4.19) and Gardnos (Norway) (age $>400\ \text{Ma}$) (Fig. 4.20). The occurrence of striking fresh PDFs in quartz exactly at the K/T boundary, a worldwide layer of ejecta from the Chicxulub structure (Mexico) (age 65 Ma) (Figs. 4.17 and 4.18), provided some of the most important initial evidence that a large meteorite impact event had occurred at that time.

In altered, geologically old, or metamorphosed samples, PDFs have an equally distinctive but discontinuous character. The original amorphous material in the PDF planes is recrystallized back to quartz, and in the process, arrays of small (typically $1\text{--}2\ \mu\text{m}$) fluid inclusions (“decorations”) develop along the original planes (Figs. 4.21 and 4.22). The resulting features, called **decorated PDFs** (Robertson *et al.*, 1968; Stöffler and Langenhorst, 1994) preserve the orientation of the original PDFs, and the distinctive shock-produced fabric can still be recognized in old rocks that have even undergone metamorphism [e.g., greenschist facies at Sudbury (Canada); Fig. 4.23]. More intense recrystallization produces arrays of small mosaic quartz crystals (**subgrains**), especially along PDFs originally parallel to the base $c(0001)$ of the quartz grain (Leroux *et al.*, 1994).

A second type of PDF, oriented parallel to the base $c(0001)$, has recently been identified, chiefly by studies of

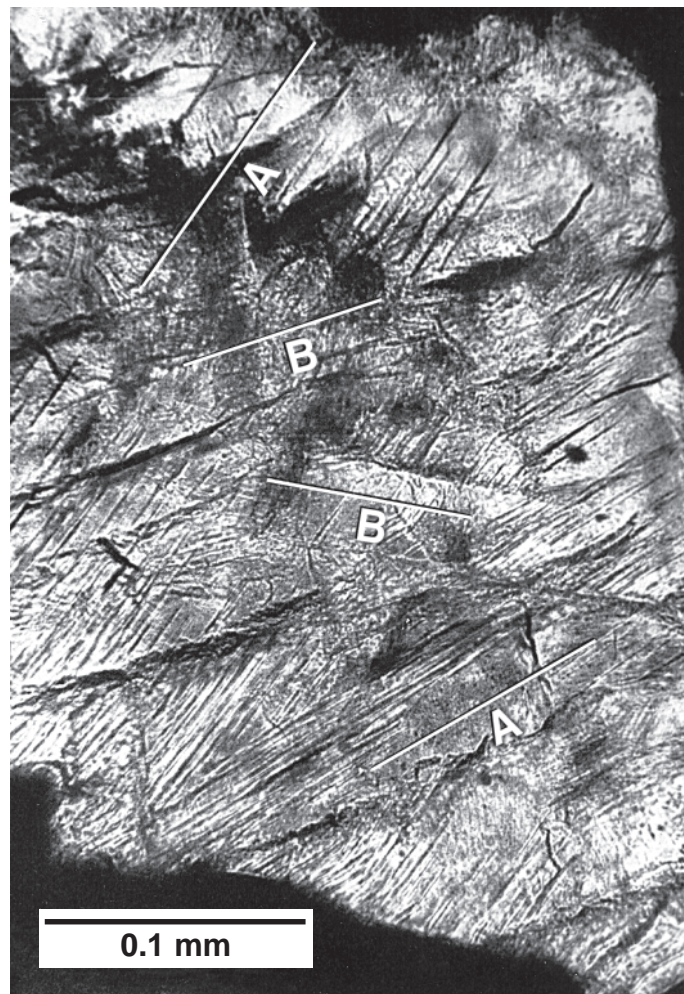


Fig. 4.16. Quartz; multiple PDFs, fresh. Striking multiple sets of PDFs developed in a quartz grain from a shocked granite inclusion in suevite from the Ries Crater (Germany). “A” indicates PDFs parallel to $\{10\bar{1}3\}$ or $\{01\bar{1}3\}$; “B” indicates PDFs parallel to $\{10\bar{1}1\}$ or $\{01\bar{1}1\}$. Note the irregular mottled extinction within the quartz grain. From *von Engelhardt and Stöffler* (1965), Fig. 1. Photograph courtesy of W. von Engelhardt (cross-polarized light).

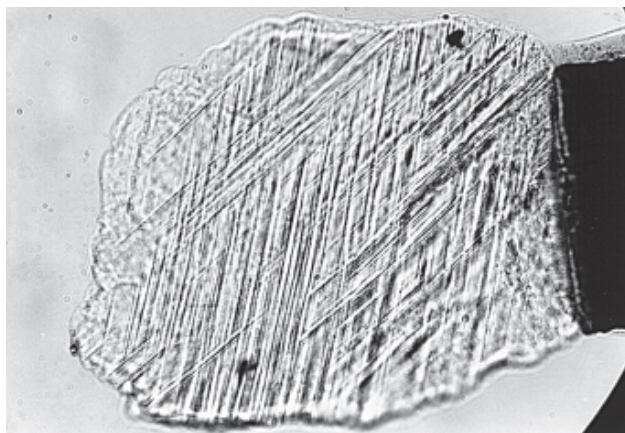


Fig. 4.17. Quartz; multiple PDFs, fresh. Small quartz grain (0.20 mm long) from K/T boundary ejecta layer, showing two prominent sets of fresh (undecorated) PDFs. (Small dots with halos are artifacts.) Specimen from Starkville South, a few kilometers south of Trinidad, Colorado. Photograph courtesy of G. A. Izett. Spindle stage mount (plane-polarized light).

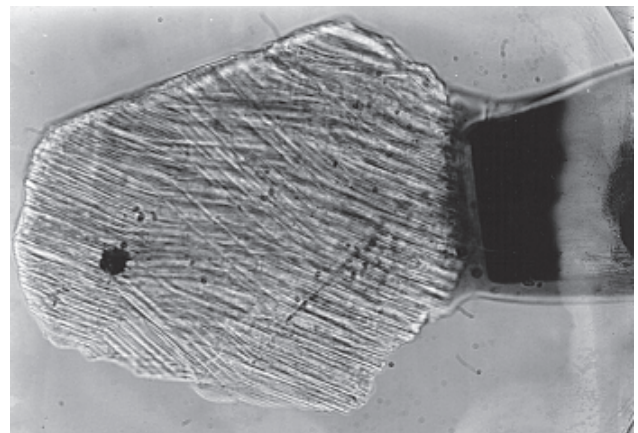


Fig. 4.18. Quartz; multiple PDFs, fresh. Small quartz grain (0.36 mm long) from K/T boundary ejecta layer, containing one opaque inclusion and multiple (3–5?) prominent sets of fresh (undecorated) PDFs. Specimen from Clear Creek North, a few kilometers south of Trinidad, Colorado. Photograph courtesy of G. A. Izett. Spindle stage mount (plane-polarized light).

TABLE 4.4. Typical crystallographic orientations of planar microstructures in shocked quartz (modified from Stöffler and Langenhorst, 1994, Table 3, p. 164).

Symbol	Miller Indexes	Polar Angle (Angle Between Pole to Plane and Quartz c-axis)
c	* (0001)	0°
ω, ω'	* {10 $\bar{1}$ 3}, {01 $\bar{1}$ 3}	23°
π, π'	* {10 $\bar{1}$ 2}, {01 $\bar{1}$ 2}	32°
r, z	* {10 $\bar{1}$ 1}, {01 $\bar{1}$ 1}	52°
m	{10 $\bar{1}$ 0}	90°
ξ	{11 $\bar{2}$ 2}, {2 $\bar{1}$ 1 $\bar{2}$ }	48°
s	{11 $\bar{2}$ 1}, {2 $\bar{1}$ 1 $\bar{1}$ }	66°
a	{11 $\bar{2}$ 0}, {2 $\bar{1}$ 1 $\bar{0}$ }	90°
	* {22 $\bar{4}$ 1}, {4 $\bar{2}$ 2 $\bar{1}$ }	77°
t	{40 $\bar{4}$ 1}, {04 $\bar{4}$ 1}	79°
k	{51 $\bar{6}$ 0}, {6 $\bar{1}$ 5 $\bar{0}$ }	90°
x	{51 $\bar{6}$ 1}, {6 $\bar{5}$ 1 $\bar{1}$ }	82°
	{6 $\bar{1}$ 5 $\bar{1}$ }, {15 $\bar{6}$ 1}	
—	{31 $\bar{4}$ 1}, {43 $\bar{1}$ 1}	78°
	{4 $\bar{1}$ 3 $\bar{1}$ }, {13 $\bar{4}$ 1}	
—	{21 $\bar{3}$ 1}, {32 $\bar{1}$ 1}	74°
	{3 $\bar{1}$ 2 $\bar{1}$ }, {12 $\bar{3}$ 1}	

*Prominent planes in typical shock fabrics.

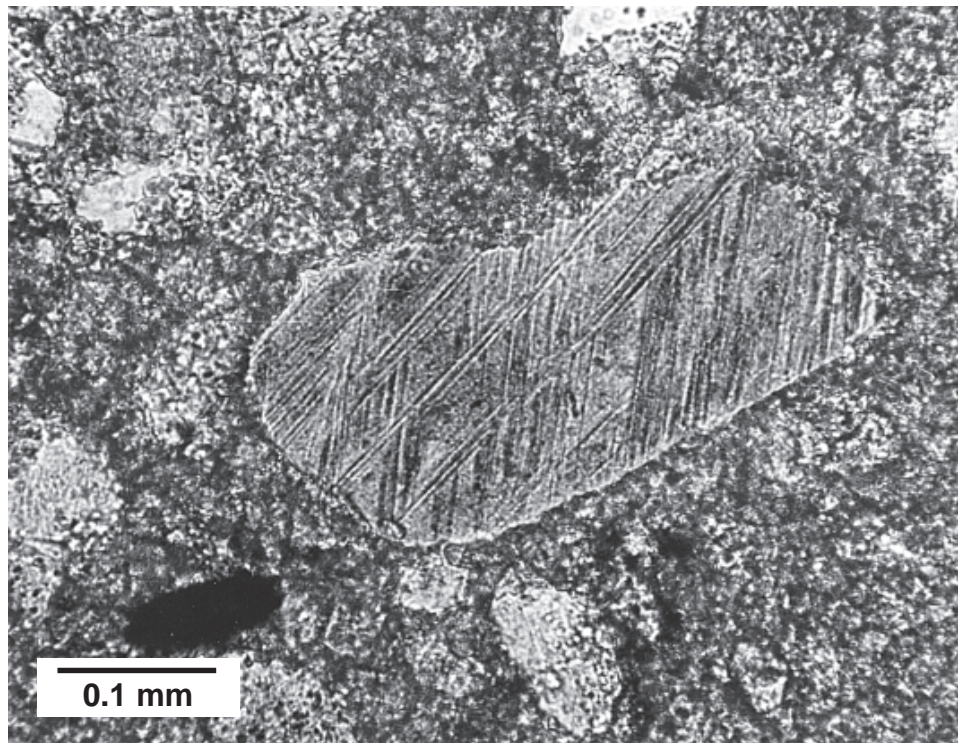


Fig. 4.19. Quartz; multiple PDFs, fresh. Shocked quartz grain containing multiple sets of fresh PDFs. The grain is included with rare sandstone fragments in a carbonate breccia dike that cuts the deformed basement rocks at Sierra Madera (Texas), an impact structure developed in a target composed dominantly of carbonate rocks. The closely spaced PDFs give a distinctive darkened, yellowish appearance to the quartz grain. Sample SMF-65-2-2 (plane-polarized light).

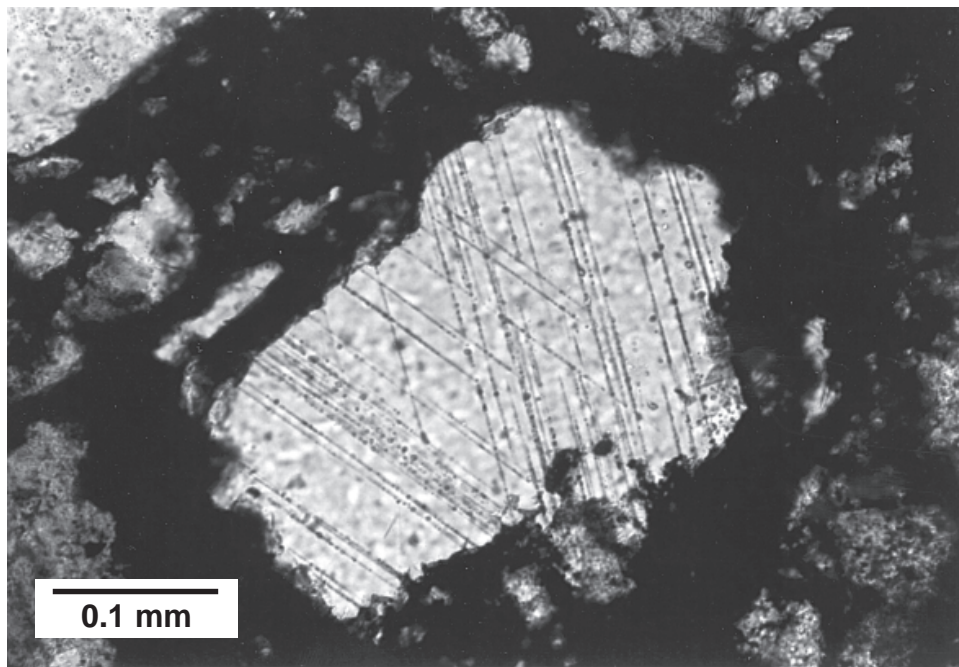


Fig. 4.20. Quartz; multiple PDFs, slightly decorated. Quartz grain in a carbon-bearing crater-fill breccia from Gardnos (Norway), showing two well-developed sets of $\{10\bar{1}3\}$ PDFs. In places, the normally continuous PDFs break down into a string of small fluid inclusions (small black dots) that follow the original trace of the PDFs. This process, by which the originally glassy material in the PDFs is recrystallized and replaced by fluid inclusions, has produced **decorated PDFs**, in which the original PDFs are visible only by the arrays of fluid inclusions that reproduce their original orientations. Sample NG-94-31 (plane-polarized light).

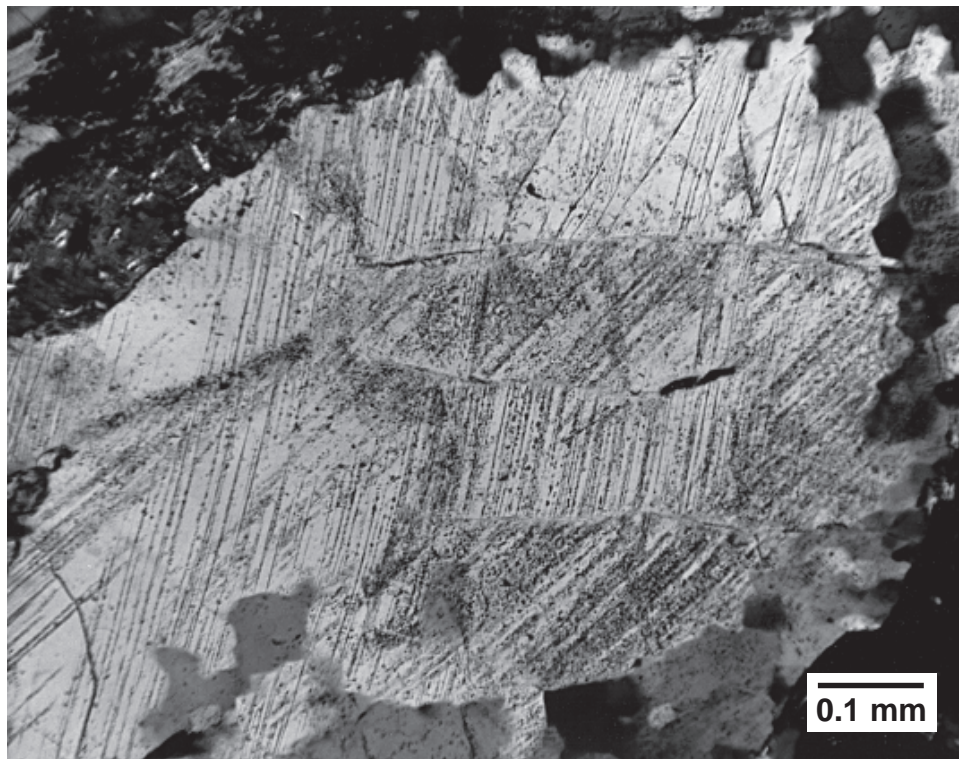


Fig. 4.21. Quartz; multiple PDFs, decorated. Large compound quartz grain from shocked basement rock inclusion in suevite breccia from Rochechouart (France), showing two prominent sets of partially decorated PDFs (north-northeast/south-southwest; northeast/southwest). Original, partly continuous PDF traces are still recognizable from the location of small fluid inclusions (black dots) along the original PDF planes. Sample FRF-69-16 (cross-polarized light).

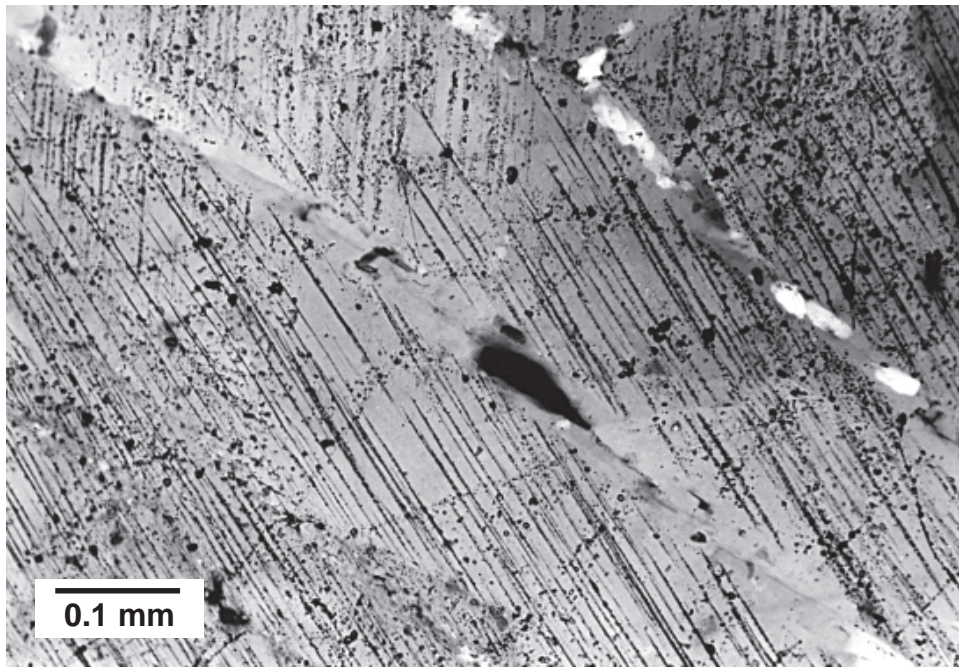


Fig. 4.22. Quartz; multiple PDFs, decorated. Compound quartz grain showing two prominent sets of decorated PDFs (north/south; northwest/southeast). The original PDF planes are now largely replaced by arrays of small fluid inclusions that preserve the original PDF orientations. Sample from Precambrian basement gneiss in the central uplift of the Carswell Lake structure (Canada). Photograph courtesy of M. R. Dence. Sample DCR-11-63B (cross-polarized light).

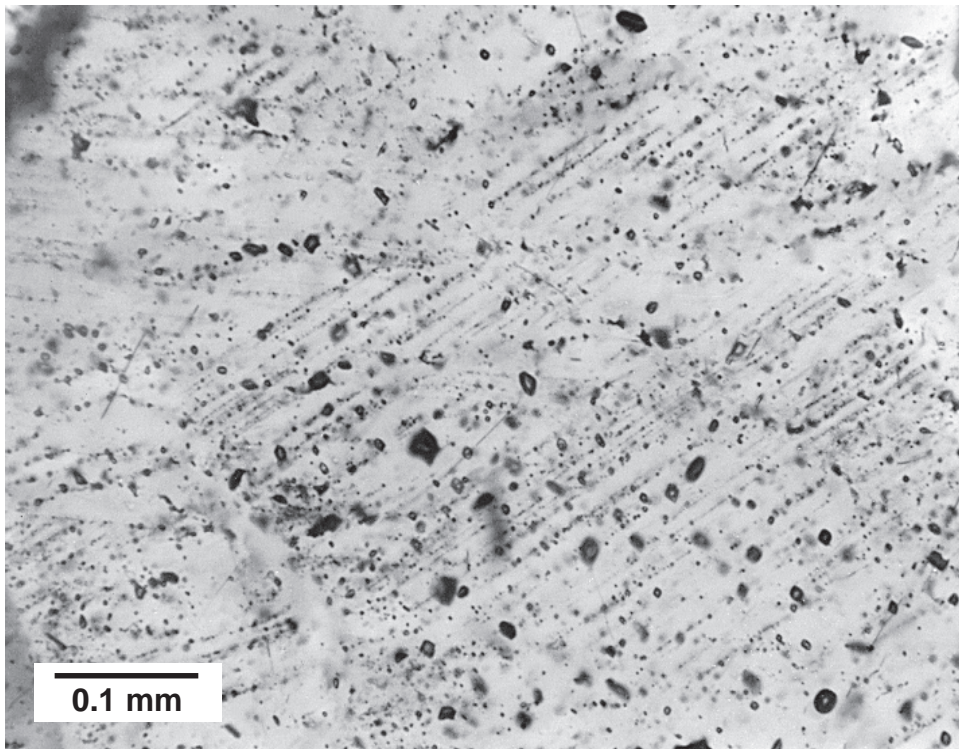


Fig. 4.23. Quartz; multiple PDFs, decorated. High-magnification view of shocked quartz from ejecta block in metamorphosed suevite, showing multiple sets of recrystallized PDFs (northwest/southeast; east/west) now expressed by arrays of small fluid inclusions (black dots). Quartz grain also contains numerous random larger fluid inclusions scattered through the grain. Sample from a small granitic gneiss inclusion in the Onaping Formation “Black Member,” from the type locality, Onaping Falls (Highway 144, Dowling Township), northwestern corner of the Sudbury structure (Canada). Photograph courtesy of N. M. Short. Sample CSF-66-39 (cross-polarized light).

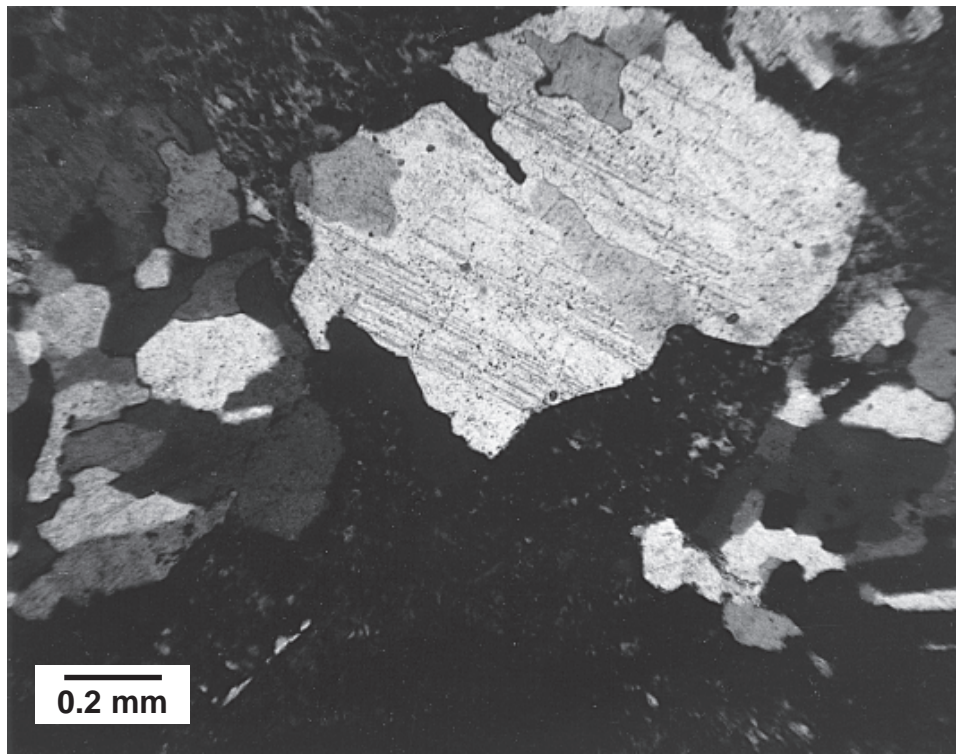


Fig. 4.24. Quartz; basal PDFs. Large irregular quartz grain associated with sericitized feldspar (dark) in footwall granitic rocks on North Range of Sudbury structure (Canada), together with shatter cones and pseudotachylite. Grain shows one well-developed set of PDFs (upper left/lower right), which appear as linear arrays of small fluid inclusions parallel to the base (0001) of the quartz grain. Sample CSF-67-55-2 (cross-polarized light).

shocked quartz with transmission electron microscopy (TEM), as **Brazil twins** (Fig. 4.24) (Leroux *et al.*, 1994; Joreau *et al.*, 1996). This form of twinning also occurs in natural unshocked quartz, but it has never been observed parallel to the base in such samples. Experimental formation of basal-oriented Brazil twins in quartz requires high stresses (about 8 GPa) and high strain rates, and it seems probable that such features in natural quartz can also be regarded as unique impact indicators (Stöffler and Langenhorst, 1994).

4.5.3. PDF Orientations

Despite the distinctive appearance of PDFs in thin section, appearance alone is not adequate to distinguish them from nonshock features or to argue that they are impact produced. An additional and definitive characteristic of PDFs is their tendency to form along specific planes in the quartz crystal lattice. Measurements of PDF orientations within the host quartz grain therefore provide a simple and reliable method to distinguish them from planar structures produced by nonshock processes. PDF orientations can be measured using standard petrofabric procedures on a U-stage (for details, measurement techniques, and specific studies, see Carter, 1965, 1968; Robertson *et al.*, 1968; von Engelhardt and Bertsch, 1969; Alexopoulos *et al.*, 1988; Stöffler and Langenhorst, 1994) or on the related spindle stage (Bloss, 1981; Medenbach, 1985; Bohor *et al.*, 1984, 1987; Izett, 1990).

The procedures involve measuring, in a single quartz grain, both the orientation of the pole (normal) to each set of PDFs

and the orientation of the c-axis (= *optic axis*) of the grain. The measurement data are then plotted on a standard stereonet, and the results are expressed as the location of the pole to the PDFs relative to the c-axis. If a large number of PDF measurements can be made on a sample, a convenient, although not entirely rigorous, method to present comparative results is to plot a frequency diagram (*histogram*) of the angles between the c-axis and the pole to each set of PDFs.

Because shock-produced PDFs in a given quartz grain are parallel to only a few specific crystallographic planes, the angles measured between the quartz c-axis and the poles to the PDFs tend to concentrate at a few specific values. In a histogram plot, the poles appear as sharp concentrations at specific angles, each of which corresponds to a particular plane (Figs. 4.25 and 4.26).

This sharply peaked pattern of PDF orientations, typically characterized by peaks at $c(0001)$ (0°), $\omega\{10\bar{1}3\}$ (23°), and $\pi\{10\bar{1}2\}$ (32°), is one of the most useful and most-used indicators of meteorite impact. Such plots clearly demonstrate the great difference between PDF distributions (Figs. 4.25a–c) and the more widely distributed, bell-shaped distribution characteristic of metamorphic deformation lamellae (Fig. 4.25e). Such plots are also used to distinguish different shock-produced fabrics that reflect different shock pressures (Fig. 4.26).

Experimental and geological studies have demonstrated that PDFs form in quartz at pressures of ~7–35 GPa, or at the lower end of the range of shock-metamorphic pressures

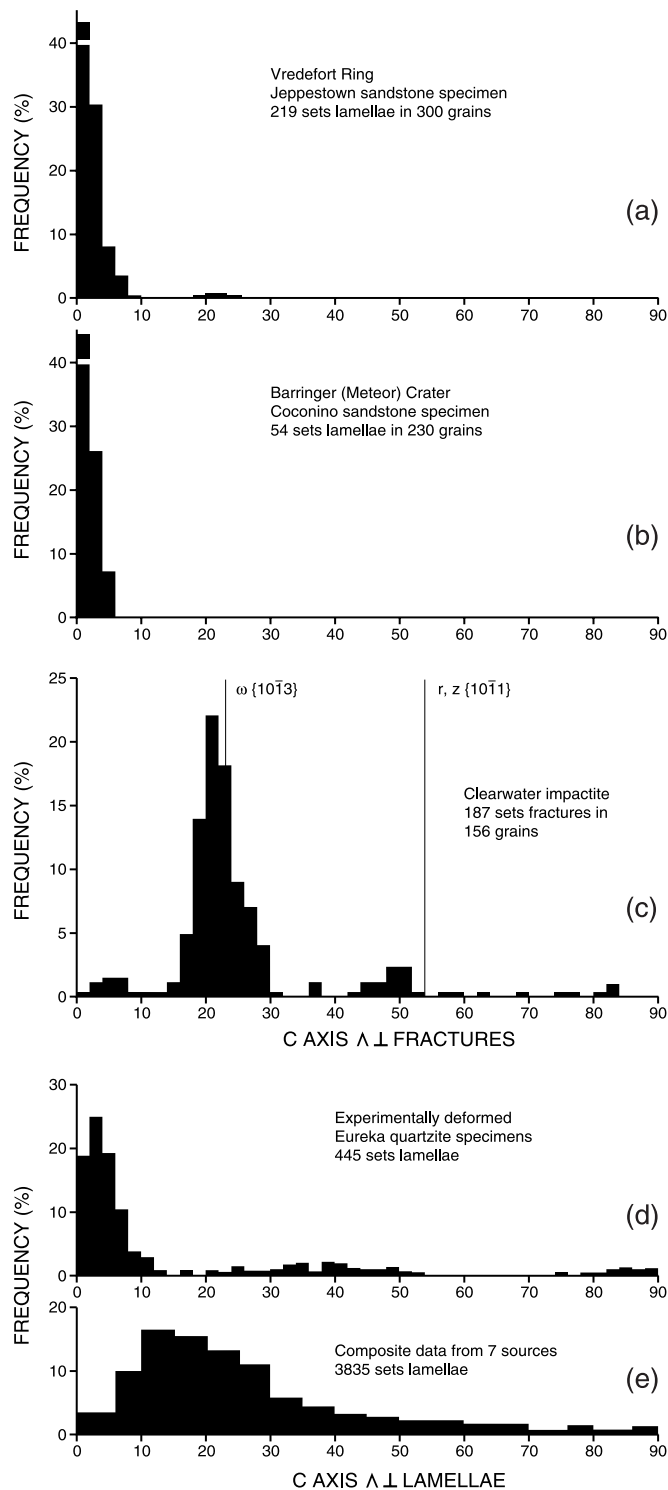


Fig. 4.25. Quartz; PDF orientations. Comparative histograms showing orientations of shock-produced PDFs and other planar deformation features in quartz (from *Carter, 1965*). In each diagram, the angle between the quartz c-axis and the pole to the planar feature is plotted on the x-axis; y-axis indicates frequency for each given angle. Shock-produced fabrics are characterized by strong orientations parallel to a few specific crystallographic planes. (a) and (b) Basal-oriented sets of deformation lamellae in shocked sandstones from the Vredefort (South Africa) and Barringer Meteor Crater (Arizona) structures; (c) distinctive PDFs showing the distinctive concentration parallel to $\omega\{10\bar{1}3\}$ [shocked crystalline rocks; Clearwater Lakes (Canada)]; (d) low-angle, near-basal fabric of deformation lamellae generated under high-strain experimental conditions; (e) broad distribution of metamorphic deformation lamellae (**Böhm lamellae**) produced by normal metamorphic conditions. The distinctive differences between shock-produced fabrics (a), (b), and (c) and those of normal metamorphism (e) have been one of the strongest arguments for the meteorite impact origin of suspected impact structures.

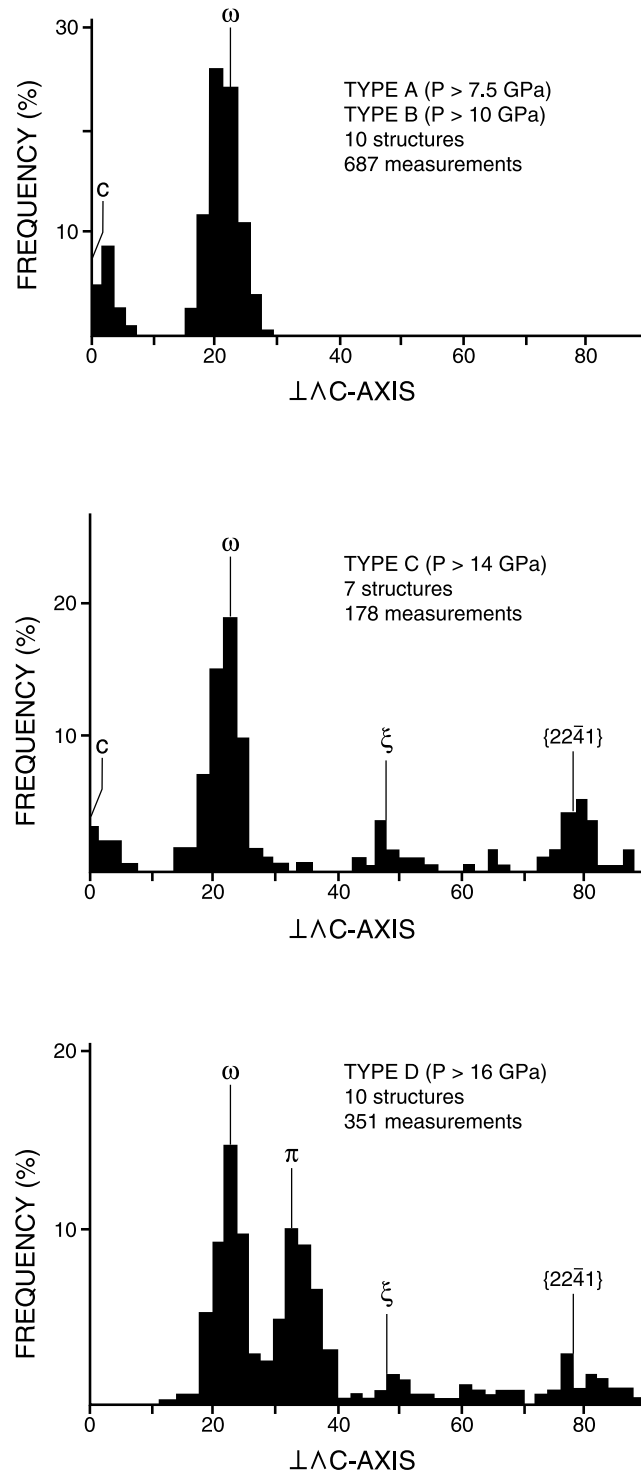


Fig. 4.26. Quartz; PDF orientations. Comparative histograms showing different fabrics displayed by PDFs in quartz produced at different shock pressures, based on measurements of shocked crystalline rocks from several Canadian impact structures (from *Robertson et al.*, 1968). With increasing shock pressures, both the total number of PDFs and the number of different orientations increase. The following fabrics, and the minimum shock pressures estimated to form them (*Grieve and Robertson*, 1976, pp. 39–40), can be recognized: *type A* ($P > 7.5$ GPa): basal PDFs only; *type B* ($P > 10$ GPa), appearance of $\omega\{10\bar{1}3\}$ planes, typically with basal planes; *type C* ($P > 14$ GPa), appearance of $\{22\bar{4}1\}$ planes with others; *type D* ($P > 16$ GPa), appearance of $\pi\{10\bar{1}2\}$ planes with others. These fabrics have been used as shock barometers to measure the intensity and distribution of shock pressures in several structures (*Grieve and Robertson*, 1976; *Robertson and Grieve*, 1977; *Dressler and Sharpton*, 1997). From *Carter* (1965).

(e.g., Hörz, 1968; Stöffler and Langenhorst, 1994). However, the relative abundance of different PDF orientations varies significantly with shock pressure. Basal Brazil twins, although little studied so far, appear restricted to shock pressures below 10 GPa. PDFs parallel to $\omega\{10\bar{1}3\}$ develop at about ≥ 7 –10 GPa, and PDFs parallel to $\pi\{10\bar{1}2\}$ at about ≥ 20 GPa. At higher pressures, e.g., 20–35 GPa, the total number of PDF sets increases, and additional orientations appear (Fig. 4.26). The PDFs formed at these higher levels tend to be intensely developed and very closely spaced within the quartz grains (Figs. 4.16, 4.18, and 4.27).

4.5.4. PDFs in Sedimentary Rocks

Although PDFs and their orientations can be reliably used as indicators of shock and impact events, it is becoming clear that our current knowledge about such features is incomplete and unrepresentative. Nearly all our information to date has come from impact structures formed in dense, coherent, quartz-bearing crystalline rocks. There is relatively little information about the effects of shock deformation in other kinds of quartz-bearing rocks, e.g., porous sandstones or fine-grained shales.

Several studies have demonstrated that shocked sandstones and shales also develop PDFs in quartz, and even diaplectic quartz and feldspar glasses, similar to those observed in shocked crystalline rocks, and these features have

been observed in sedimentary rocks from several impact structures (Kieffer, 1971; Kieffer *et al.*, 1976a; Grieve *et al.*, 1996).

Despite these similarities, a growing amount of data now indicates that sedimentary rocks, especially porous ones, respond differently to shock waves than do nonporous crystalline rocks. One indication of significant differences is that PDF fabrics measured in sediments show a large proportion of PDFs whose poles are oriented at high angles ($>45^\circ$) to the quartz *c*-axis (Grieve *et al.*, 1996; Gostin and Theriault, 1997). Other possible differences are that PDFs may first appear, or a particular PDF fabric may develop, at different shock pressures in sedimentary rocks than in crystalline rocks.

A more important difference between porous and nonporous rocks is that a shock wave passing through porous sediments will generate more heat than in passing through crystalline rocks, chiefly because more of the shock-wave energy is absorbed by the numerous grain interfaces and pore spaces in the sediment (Kieffer, 1971; Kieffer *et al.*, 1976a; Kieffer and Simonds, 1980; Stöffler, 1984). As a result, extensive melting will occur at lower shock pressures in sediments than in crystalline rocks, i.e., at about 15–20 GPa in sandstone vs. 50–60 GPa in crystalline rocks (Stöffler, 1972, 1984). Therefore, the higher-pressure fabrics of quartz PDFs, which form at 20–30 GPa in crystalline rocks, may not be found in sediments, either because they did not form or because they

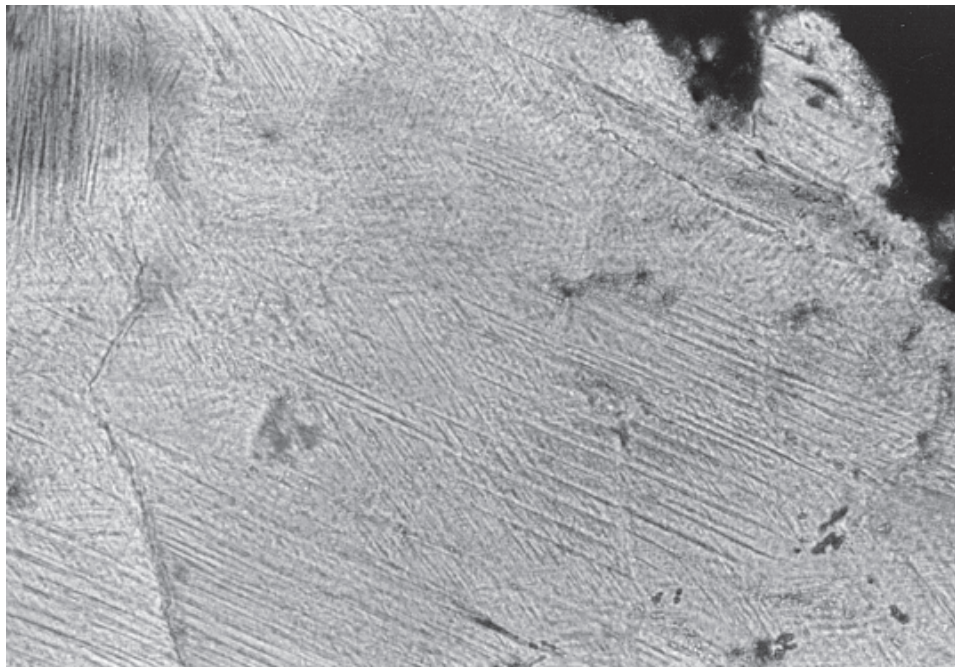


Fig. 4.27. Quartz; multiple PDFs, fresh. Photomicrograph showing at least four sets of fresh PDFs in a shocked quartz grain from crystalline target rocks at the Lake St. Martin impact structure, Manitoba (Canada). Two prominent PDF sets (northwest/southeast and west-northwest/east-southeast) are accompanied by less obvious sets oriented approximately north/south and east/west. Petrofabric measurements with a U-stage show that the PDFs are oriented parallel to both $\omega\{10\bar{1}3\}$ and $\pi\{10\bar{1}2\}$, indicating moderately high shock pressures (>15 GPa). Patches of diaplectic glass, associated with the shocked quartz, appear as dark zones (e.g., upper right). Width of field is ~ 100 μm . Photograph courtesy of V. L. Sharpton (cross-polarized light).

were immediately destroyed by postshock melting. The unique shock effects observed in sedimentary rocks can still provide conclusive evidence for an impact origin [e.g., at Barringer Meteor Crater (Arizona) (Kieffer, 1971)], but the details of such occurrences cannot be accurately interpreted on the basis of results from shocked nonporous crystalline rocks (Grieve *et al.*, 1996).

4.6. PLANAR MICROSTRUCTURES IN FELDSPAR AND OTHER MINERALS

Similar planar microstructures are produced by shock in many other minerals (e.g., Stöffler, 1972, 1974), but such features have been less used as indicators of meteorite impact. Feldspars of all kinds (both alkali varieties and plagioclase) display various shock-produced planar microstructures: fractures, deformation bands, kink bands, and actual PDFs. Frequently, short and closely spaced PDFs may be combined with longer and more widely spaced features (deformation bands or albite twinning) to produce a distinctive **ladder texture** (Figs. 4.28, 4.29, and 4.30).

Although several studies have been made of shock-produced planar features in feldspars (e.g., Stöffler, 1967, 1972; papers in French and Short, 1968), these features have been less studied and less well characterized than those in quartz. There are several reasons for this: the greater diversity and complexity of such features, the greater optical complexity (*biaxial*) of feldspars, and the common secondary alteration of the feldspar and its planar features to clays, iron oxides, etc. (Figs. 4.29 and 4.30). Another factor in studies focused on identifying new impact structures is the fact that shocked feldspar in crystalline rocks is generally associated with shocked quartz, whose features (especially PDFs) provide a quicker and simpler method for establishing an impact origin.

Planar microstructures, both planar fractures and true PDFs, have also been observed in other minerals, including pyroxene, amphiboles, and several accessory phases (apatite, sillimanite, cordierite, garnet, scapolite, and zircon) (Stöffler, 1972). Less is known about PDF formation and orientations in these minerals, because appropriate rocks are less abundant in most impact structures, and because the specific minerals have not been studied in detail. However, recognition of shock-produced PDFs in zircon has been especially important in applying U-Th-Pb dating methods to individual zircons in shocked target rocks to determine the ages of impact structures (e.g., Krogh *et al.*, 1984, 1993; Kamo and Krogh, 1995).

The development of distinctive shock-metamorphic features such as PDFs in denser mafic minerals like amphibole, pyroxene, and olivine apparently occurs at higher pressures and over a more limited pressure range than in quartz and feldspar. At pressures <30 GPa, sufficient to form PDFs in both quartz and feldspar, the most common shock effects observed in mafic minerals are planar fractures, mechanical twins, and general comminution (Stöffler, 1972); features

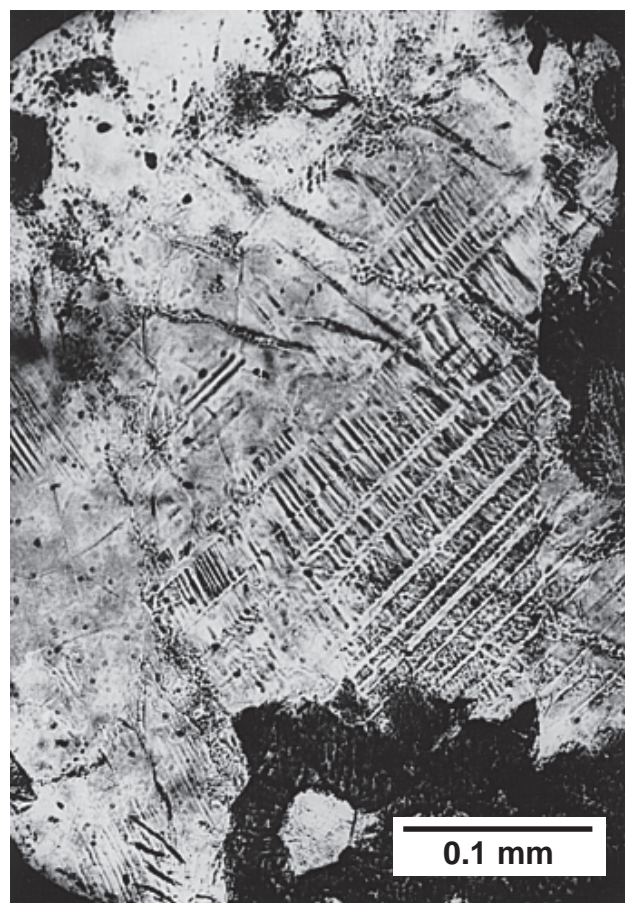


Fig. 4.28. Feldspar; multiple PDFs and diaplectic glass (maskelynite). Shocked plagioclase feldspar grain from the Ries Crater (Germany), showing development of multiple sets of PDFs (lower right) and gradational conversion of the same crystal to diaplectic glass (**maskelynite**) (upper left). Original polysynthetic albite twin lamellae (northwest/southeast) are still preserved in part of the crystal (lower right), but alternate twin lamellae have either been converted to maskelynite (clear) or are crosscut by short, closely spaced PDFs to form a distinctive “ladder” structure. Elsewhere in the crystal (upper left), both the original twins and the subsequent shock-produced PDFs disappear, and the whole crystal consists of maskelynite. Sample from a moderately shocked amphibolite fragment in suevite breccia. From Stöffler (1966), Fig. 4 (plane-polarized light).

resembling true PDFs are only rarely observed. At higher pressures, mafic minerals in naturally and experimentally shocked basalts generally show only extreme comminution, accompanied by the melting and flow of associated feldspar (Kieffer *et al.*, 1976b; Schaal and Hörz, 1977). PDFs are therefore unlikely to be observed in mafic minerals in impact structures. The higher pressures apparently required for their formation imply that they will form in a correspondingly smaller volume of shocked rock in the structure. Furthermore, the higher shock pressures required are closer to pressures that produce partial to complete melting of the rock, so that PDFs, even if formed, would not survive any subsequent melting episode.

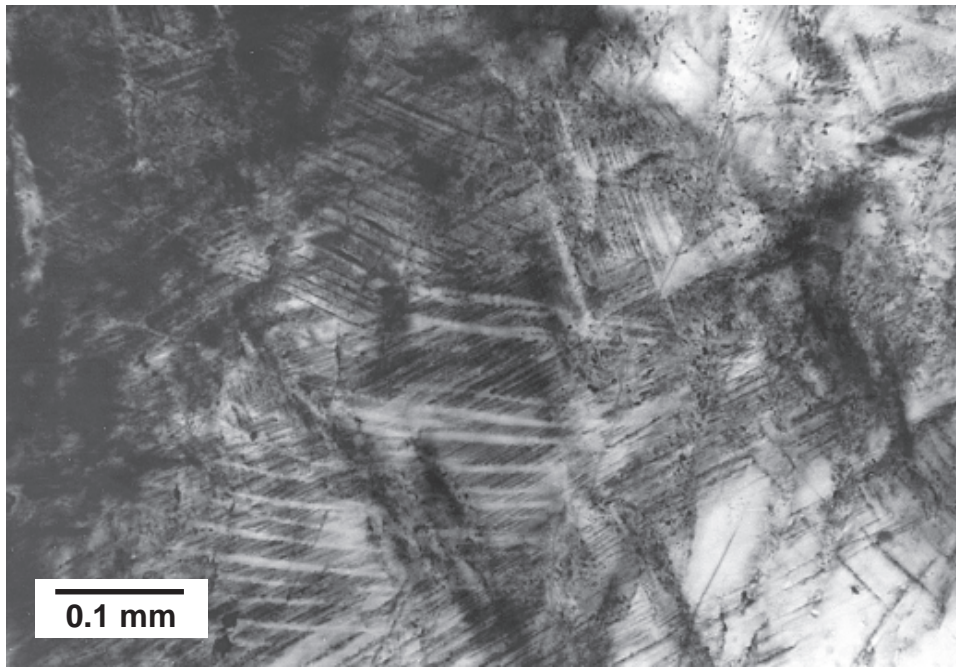


Fig. 4.29. Feldspar; multiple PDFs, “ladder” texture. Shocked K-feldspar, showing multiple sets of altered PDFs. Two types of planar deformation features are present: (1) long, thicker, widely spaced planes (clear areas, approximately east/west) that may be deformation bands or kink bands; (2) short, narrower, closely spaced features (northeast/southwest and north-northwest/south-southeast) that combine with the first type to form a distinctive “ladder” texture. The planar features have a brownish-red color, possibly caused by alteration of the feldspar to clay minerals and iron oxides. Sample from a small granitic gneiss inclusion in the Onaping Formation “Black Member” from the type locality, Onaping Falls (Highway 144, Dowling Township), northwestern corner of the Sudbury structure (Canada). Photograph courtesy of N. M. Short. Sample CSF-66-39 (cross-polarized light).

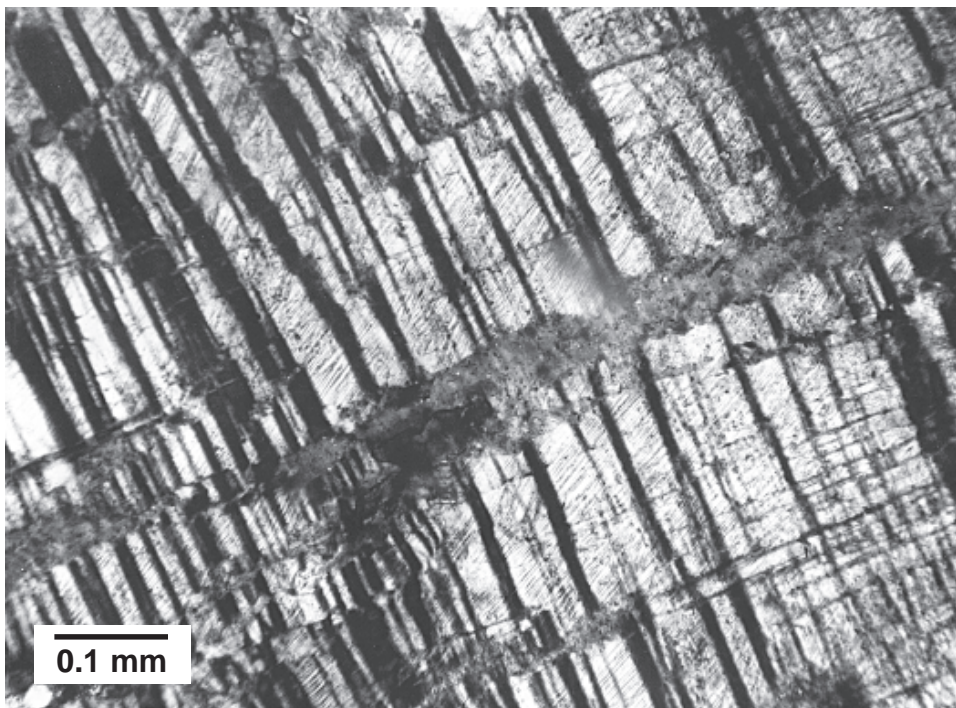


Fig. 4.30. Feldspar; twinning and PDFs. Large deformed feldspar crystal (microcline?) in granitic fragment in suevite breccia. Original twinning in the feldspar (light/dark pattern, northwest/southeast) is deformed and faulted along multiple parallel fractures (east-northeast/west-southwest). Elsewhere, the feldspar is cut by a single set of short, narrow, closely spaced planar features (northeast/southwest) that may be actual PDFs. Sample from a small block of granitic gneiss from the Onaping Formation “Black Member,” Sudbury (Canada). Sample CSF-67-73 (cross-polarized light).

4.7. SHOCK ISOTROPIZATION AND DIAPLECTIC GLASSES

Planar microstructures form at relatively low shock pressures (>7 – 35 GPa) (Table 4.2) (Stöffler and Langenhorst, 1994) and involve only partial and localized deformation of the host crystal. PDFs, which develop in the upper part of this range (10 – 35 GPa), involve actual conversion of the quartz crystal structure to an amorphous phase within the individual planes. Higher shock pressures (35 – 45 GPa), which transmit more energy into the crystal, do not form PDFs. Instead, the shock waves convert the entire crystal to an amorphous (glassy) phase.

This shock-produced **diaplectic glass** (also called **thetomorphonic glass**) (Stöffler, 1966, 1967, 1972, 1984; Chao, 1967; papers in French and Short, 1968) is completely different from conventional glasses produced by melting a mineral to a liquid at temperatures above its melting point. Diaplectic glasses do not melt or flow; they preserve the original textures of the crystal and the original fabric of the mineral in the rock. In addition, although diaplectic glasses are optically isotropic (i.e., they show no birefringence when examined petrographically under crossed polarizers), studies of quartz and feldspar diaplectic glasses by X-ray diffraction and infrared spectrometry have shown that they retain much of the ordered atomic structure of the original crystal (e.g., Bunch *et al.*, 1967, 1968; Stöffler, 1974, 1984; Arndt *et al.*, 1982).

Samples of diaplectic feldspar glasses have also been experimentally annealed by heating at ambient pressure to produce original single crystals (Bunch *et al.*, 1967, 1968; Arndt *et al.*, 1982) or microcrystalline aggregates that preserve the shapes of the original feldspar crystals (Arndt *et al.*, 1982; Ostertag and Stöffler, 1982).

Quartz and feldspar are the most common examples of minerals converted to diaplectic glasses by shock waves. Diaplectic plagioclase feldspar glass, called **maskelynite**, was in fact observed in meteorites more than a century before it was discovered in shocked terrestrial rocks. The same material, often well preserved, is also observed at several impact structures where highly shocked rocks are preserved, e.g., the Ries Crater (Germany) (Figs. 4.28, 4.32, and 4.33) and Manicouagan (Canada) (Fig. 4.31).

In these occurrences, the unique textures of the diaplectic glasses clearly indicate formation without melting to the liquid state. The overall grain fabric of the rock is unchanged, and the diaplectic glasses preserve the shapes of the original quartz and feldspar grains. In some grains, the transformation to diaplectic glass is incomplete, and areas of relict birefringence remain in the otherwise isotropic material (Figs. 4.28 and 4.31). In some shocked plagioclase grains, one set of alternating albite twins is converted to maskelynite, while the twins of the other set remain birefringent. Other minerals (e.g., amphibole, garnet, micas), associated with (or even in contact with) grains of diaplectic glass, show little

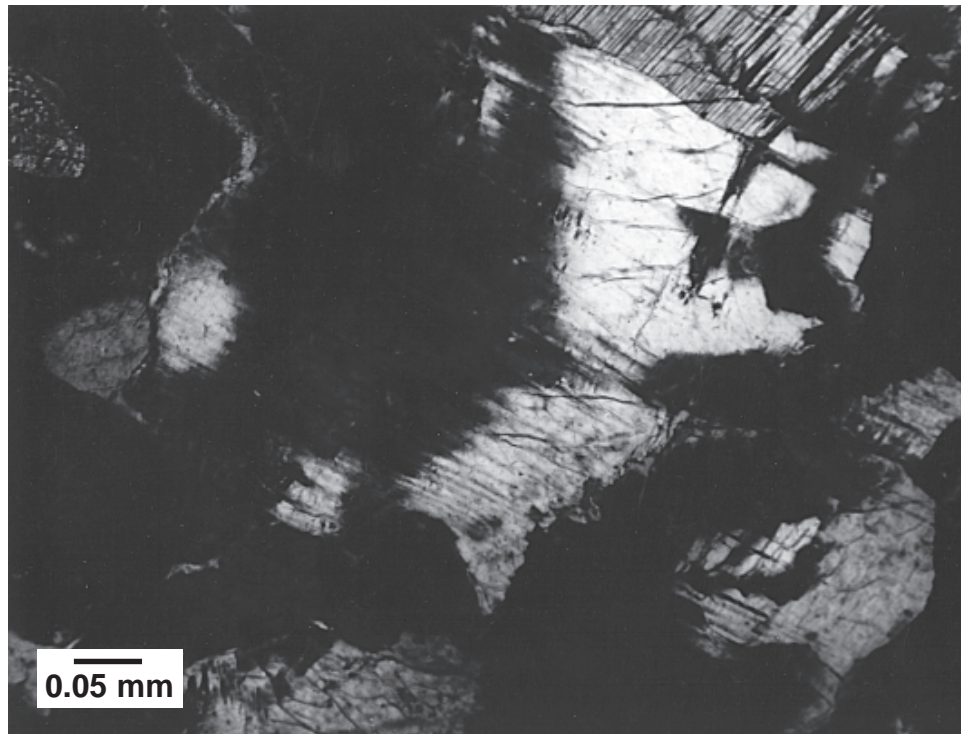


Fig. 4.31. Feldspar; diaplectic glass (maskelynite). Shocked plagioclase feldspar, partially converted to isotropic diaplectic feldspar glass (maskelynite). Parts of the original coarse feldspar grains remain crystalline and birefringent (light areas); these regions grade into adjoining areas of maskelynite (dark). Drill-core sample from coarse-grained basement anorthosite, exposed in the central uplift of the Manicouagan structure (Canada). Photograph courtesy of M. R. Dence. Sample DMM-73-63B (cross-polarized light).

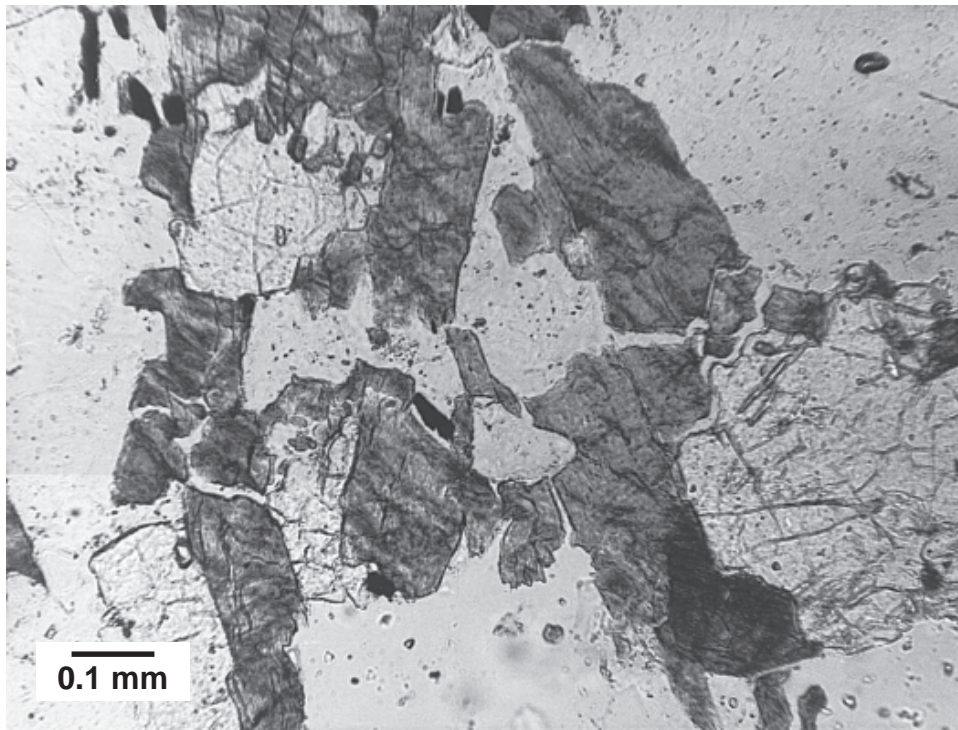


Fig. 4.32. Feldspar and quartz; diaplectic glasses. Biotite gneiss containing diaplectic feldspar glass (maskelynite) (clear, low relief; e.g., upper right) and diaplectic quartz glass (clear, higher relief, e.g., lower right). The associated biotite crystals (dark) have retained their original shape and have remained crystalline and birefringent, despite the complete transformation of adjacent quartz and plagioclase into glassy phases (compare with Fig. 4.33). Biotite gneiss inclusion in suevite breccia, Otting, Ries Crater (Germany). From *Stöffler* (1967), Fig. 12a. Photograph courtesy of D. Stöffler (plane-polarized light).

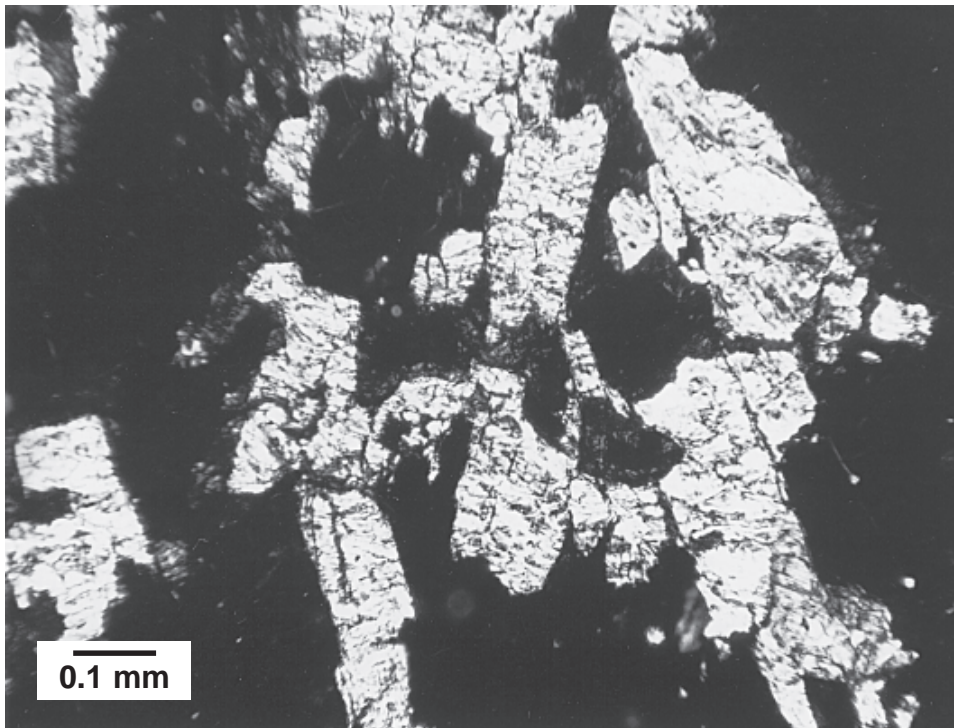


Fig. 4.33. Feldspar and quartz; diaplectic glasses. Biotite gneiss containing diaplectic feldspar glass (maskelynite) and diaplectic quartz glass (compare with Fig. 4.32). Both phases are isotropic (dark) under crossed polarizers. The associated biotite crystals have retained their original shape and have remained crystalline and birefringent, despite the complete transformation of adjacent quartz and plagioclase into glassy phases. Biotite gneiss inclusion in suevite breccia, Otting, Ries Crater (Germany). From *Stöffler* (1967), Fig. 12b. Photograph courtesy of D. Stöffler (cross-polarized light).

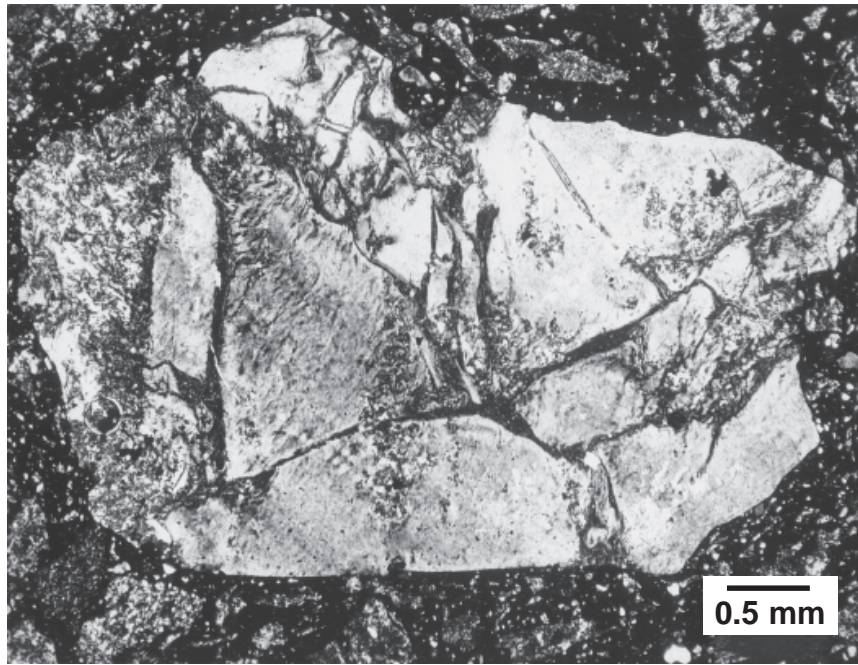


Fig. 4.34. Feldspar; possible diaplectic glass, recrystallized. Large, highly deformed and recrystallized feldspar clast in suevite breccia, surrounded by finer fragments in an opaque carbon-bearing matrix. The feldspar shows deformation and recrystallization throughout, as indicated by the intensely mosaic extinction. The crystal is subdivided by thin irregular zones of nearly isotropic material, possibly original melt. Plastic behavior of the fragment is also suggested by indentations of the matrix into the clast (e.g., at top). This clast can be interpreted as a fragment of diaplectic feldspar glass that has subsequently been recrystallized to form a fine-grained microcrystalline texture that is still similar to the original crystal. Similar reactions have been produced in experimentally annealed maskelynite. Another possibility is that the fragment was shock-heated above its melting point, but was rapidly quenched (perhaps during deposition) before extensive flow could occur. In any case, the unusual texture has been preserved despite subsequent metamorphism of the unit in which it occurs. Fragment in Onaping Formation “Black Member” from type locality, Onaping Falls (Highway 144, Dowling Township), northwestern corner of Sudbury structure (Canada). Sample CSF-66-37-2 (cross-polarized light).

deformation and retain their original form (Figs. 4.32 and 4.33), although they may show reduced birefringence and reddening produced by the formation of hematite (e.g., *Feldman*, 1994) and cordierite (*Stähle*, 1973).

Diaplectic glasses formed from other minerals (e.g., scapolite) have rarely been observed. Mafic minerals (e.g., pyroxene, amphibole, and biotite) do not seem to form diaplectic glasses, probably because the pressures required are higher than those for quartz and feldspar, high enough so that shock-produced melting occurs instead.

Diaplectic quartz and feldspar glasses are metastable. They apparently do not survive if they are exposed to even relatively mild postimpact thermal effects. Diaplectic glasses are not observed in impact structures that have been even slightly metamorphosed, even though decorated PDFs may still be preserved in associated quartz. In such settings, instead of diaplectic glasses, one observes quartz and feldspar grains that are recrystallized to microcrystalline aggregates that replace the original crystal (Figs. 4.34, 4.35, and 4.36). Textures in the altered feldspars sometimes suggest intense plastic deformation and flow within the original grain. These features are often accompanied by the development of plumose or spherulitic microcrystalline textures that may reflect significant thermal effects as well. Such grains of quartz and

feldspar have been tentatively interpreted as original diaplectic glasses that have been annealed and recrystallized, either by immediate postshock thermal effects or by subsequent metamorphism (*McIntyre*, 1968; *French*, 1968b, pp. 401–404).

4.8. SELECTIVE MINERAL MELTING

The high-pressure (35–45 GPa) shock waves that produce diaplectic glasses also generate significant and sudden postshock temperature rises of several hundred degrees Celsius in the rocks and minerals through which they pass (Fig. 4.1). In the region of diaplectic glass formation, postshock temperatures are still low enough (300°–900°C) that virtually no actual melting occurs, and rapidly quenched samples of diaplectic glasses suffer no further immediate alteration. However, at slightly higher shock pressures (~45–50 GPa), the higher postshock temperatures ($\geq 1000^\circ\text{C}$) begin to exceed the melting points of typical rock-forming minerals, and distinctive localized melting effects appear in the affected rocks.

This shock-produced **selective mineral melting** differs significantly from normal equilibrium melting. Under nor-

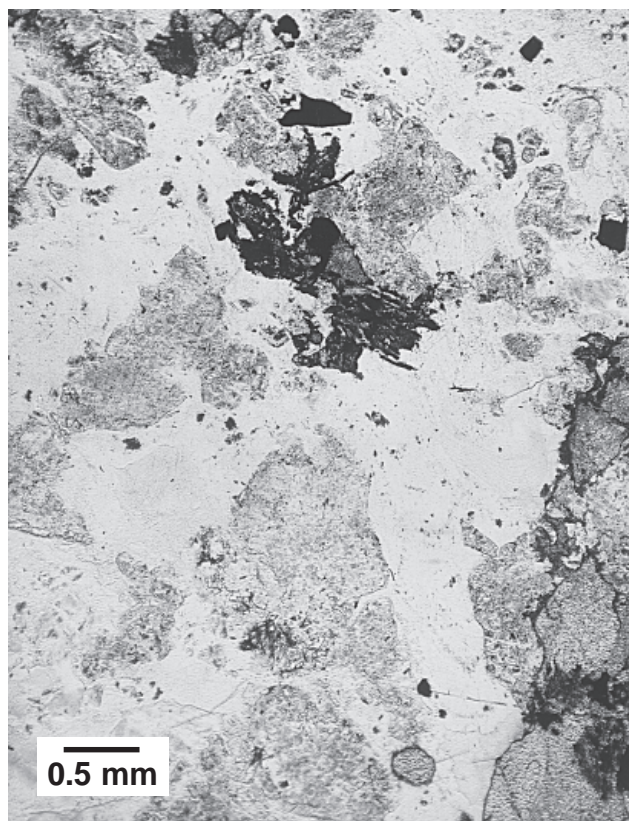


Fig. 4.35. Feldspar; possible diaplectic glass, recrystallized. Shock-deformed and recrystallized feldspar and quartz from a coarse-grained granitic fragment in suevite breccia. Large original quartz grains (lower center; gray, higher relief) are recrystallized to finely crystalline mosaic quartz. Original feldspar grains (clear, lower relief) are generally finely recrystallized and virtually isotropic in some areas (compare with Fig. 4.36), although some areas of original feldspar crystals are preserved. From granitic inclusion in Onaping Formation “Black Member” at type locality, Onaping Falls (Highway 144, Dowling Township), northwestern corner of Sudbury structure (Canada). Sample CSF-66-50-13 (plane-polarized light).

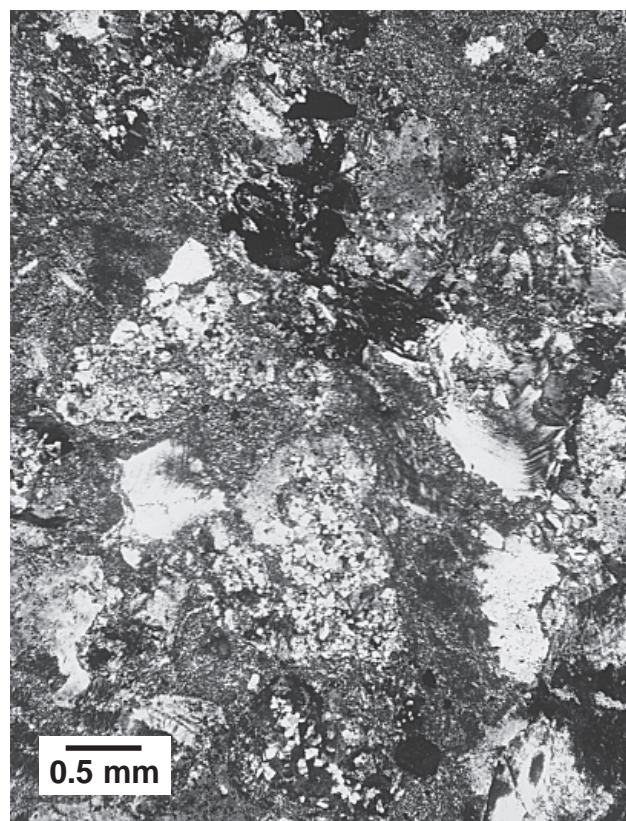


Fig. 4.36. Feldspar; possible diaplectic glass, recrystallized. Shock-deformed and recrystallized feldspar and quartz from a granitic fragment in suevite breccia. Large original quartz grains are recrystallized to finely crystalline mosaic quartz. Original feldspar grains are generally finely recrystallized and virtually isotropic in some areas, although some areas of original feldspar crystals are preserved (compare with Fig. 4.35). In one such area (right center), a plagioclase crystal has been plastically deformed, bending the original polysynthetic albite twinning (light/dark bands) through a large angle. Despite the intense deformation of quartz and feldspar, a single apatite grain (lower right) shows no deformation. Sample from granitic inclusion in Onaping Formation “Black Member” at type locality, Onaping Falls (Highway 144, Dowling Township), northwestern corner of Sudbury structure (Canada). Sample CSF-66-50-13 (cross-polarized light).

mal conditions of increasing overall temperature, melting occurs first at the boundaries between different mineral grains. Two or more different minerals are involved, and the resulting *eutectic* melt has a composition intermediate between that of the adjacent minerals and forms at a temperature well below that of their individual melting points. In a shock-wave environment, each mineral grain is instantaneously raised to a postshock temperature that depends on the shock-wave pressure and on the density and compressibility of the mineral itself. If the postshock temperature produced in a mineral exceeds its normal melting temperature, each grain of that mineral in the rock will melt, immediately and independently, after the shock wave has passed. The melt will have approximately the same composition as the origi-

nal mineral before any flow or mixing takes place, and the melt regions will initially be distributed through the rock in the same pattern as the original mineral grains.

Selective melting therefore produces unusual textures in which one or more minerals in a rock show typical melting features while others — even immediately adjacent ones — do not. Shocked granitic inclusions from the Ries Crater (Germany) frequently show a texture in which feldspar has melted, flowed, and vesiculated, but the adjacent quartz remains in the form of unmelted diaplectic glass (*Chao*, 1967; *Stöffler*, 1972, 1984). Similar textures can be preserved even in subsequently metamorphosed rocks, in which flowed and recrystallized feldspar is accompanied by recrystallized but undeformed grains of quartz (Fig. 4.37).

At higher shock pressures, where temperatures are higher and cooling times may be longer, these selective melting textures may be complicated by the effects of normal eutectic melting at grain boundaries (Fig. 4.37). In some shocked rocks, postshock temperatures may exceed the melting points of all the minerals present, and the rock will melt to a mixture of heterogeneous glasses that may preserve (depending on the amount of subsequent flow and mixing) the original shapes and mineral compositions. If such rocks are quenched before flow and mixing can occur, the chemically diverse glasses can survive and be recognized, even after significant metamorphism (Fig. 4.38) (Peredery, 1972).

Such distinctive selective melting textures are relatively uncommon in rocks from impact structures. The region of shock pressures that produces them is relatively narrow (~45–55 GPa), and their preservation, once formed, requires rapid quenching, most commonly as small inclusions in crater-fill breccias. At progressively higher shock pressures (≥ 55 GPa), postshock temperatures increase rapidly, melting becomes complete, flow and mixing processes become dominant in the melted rock, and more chemically homogeneous bodies of **impact melt** are produced (see Chapter 6).

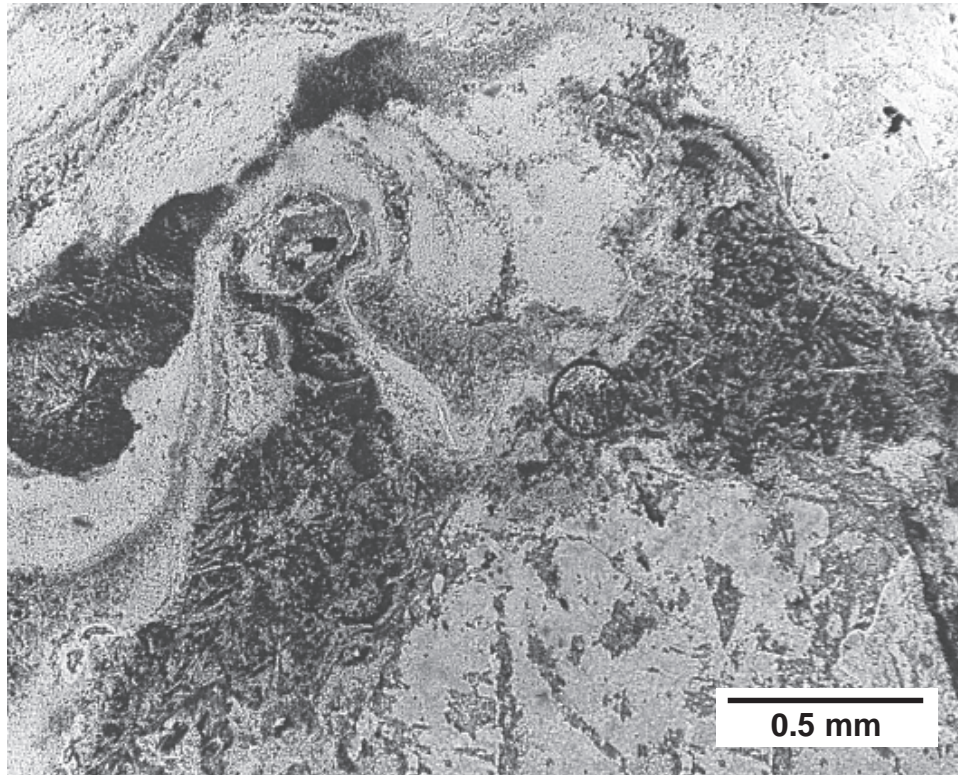


Fig. 4.37. High-temperature effects; plastic deformation, grain-boundary melting. Highly shocked and recrystallized quartzofeldspathic inclusion in metamorphosed suevite breccia, showing extreme deformation of quartz and feldspar. Quartz (gray, higher relief, lower right) is recrystallized to a fine mosaic of small quartz grains. Feldspar (clear, lower relief, top) shows intense, contorted flow structure, indicating either incipient melting or extreme plastic flow. Definite incipient melting has occurred at the grain boundaries, forming a brown melt (dark) with lath-like microlites (white; feldspar?). (Circular feature at center is a bubble in the thin section.) Coarse-grained granitic inclusion in Onaping Formation “Black Member,” Sudbury structure (Canada). Sample CSF-67-67 (plane-polarized light).

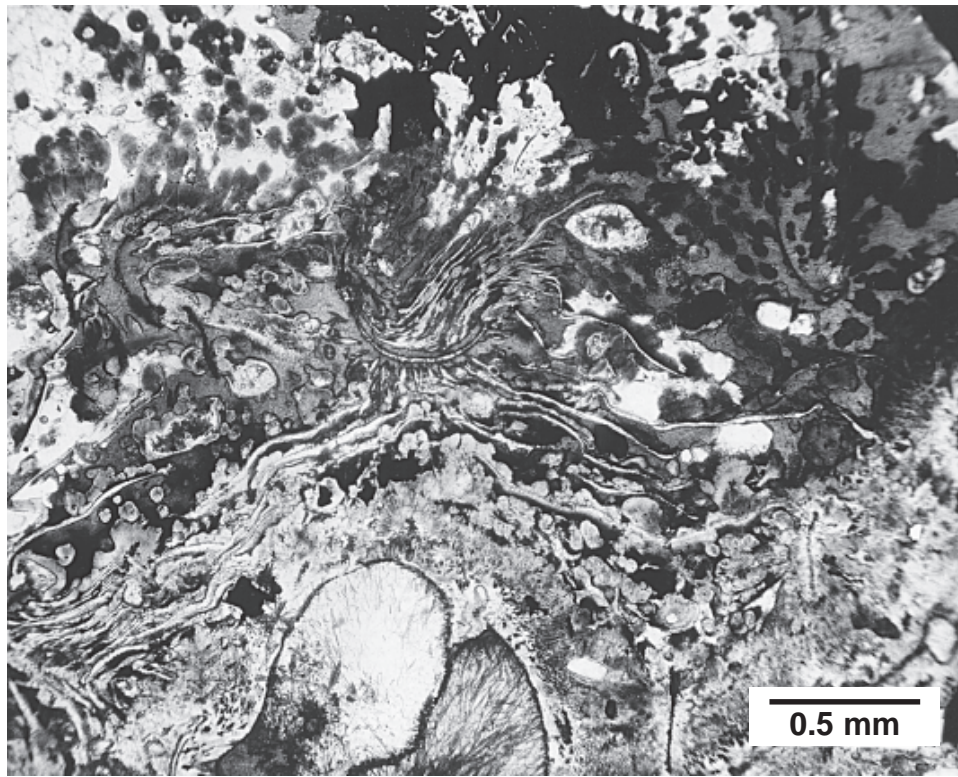


Fig. 4.38. High-temperature effects; complete melting. Highly shocked, melted, and recrystallized rock inclusion in metamorphosed suevite breccia. Postshock temperatures apparently exceeded the melting points of all component minerals, converting the originally crystalline rock into an initially heterogeneous glass that developed limited flow textures before it was quenched. The inclusion was subsequently recrystallized to secondary minerals such as quartz, feldspar, amphibole, and chlorite, but the original mineralogy and the character of the shock-formed heterogeneous glass are still detectable in the distribution and chemical variations in the secondary mineral assemblage. Inclusion in Onaping Formation “Black Member” at the type locality, Onaping Falls (Highway 144, Dowling Township), northwestern corner of Sudbury structure (Canada). Sample CSF-66-50-3 (plane-polarized light).